МІНІСТЕРСТВО ОСВІТИ ТА НАУКИ УКРАЇНИ
НАЦІОНАЛЬНИЙ АВІАЦІЙНИЙ УНІВЕРСИТЕТ
КАФЕДРА КОНСТРУКЦІЇ ЛІТАЛЬНИХ АПАРАТІВ

ДОПУСТИТИ ДО ЗАХИСТУ
Завідувач кафедри, д.т.н., проф.
_____ Сергій ІГНАТОВИЧ
«____» _____ 2021 р.

ДИПЛОМНА РОБОТА
ВИПУСКНИКА ОСВІТНЬОГО СТУПЕНЯ «МАГІСТР»
ЗІ СПЕЦІАЛЬНОСТІ:
«АВІАЦІЙНА ТА РАКЕТНО-КОСМІЧНА ТЕХНІКА»

Тема: «Розробка системи керування граничним шаром крила надлегкого літака на основі плазмових актуаторів»

Виконавець: _____ **Валентин МАТВІЄНКО**

Керівник: к.т.н., доц. _____ **Вадим ЗАКІЄВ**

Консультанти з окремих розділів пояснювальної записки:
охорона праці:
к.біол.н., доц. _____ **Вікторія КОВАЛЕНКО**

охорона навколишнього середовища:
к.г.-м.н., доц. _____ **Тамара ДУДАР**

Нормоконтролер: к.т.н, доц. _____ **Сергій ХИЖНЯК**

Київ 2021

MINISTRY OF EDUCATION AND SCIENCE OF UKRAINE
NATIONAL AVIATION UNIVERSITY
DEPARTMENT OF AIRCRAFT DESIGN

PERMISSION TO DEFEND
Head of the department,
Professor, Dr. of Sc.
_____ Sergiy IGNATOVYCH
«___» _____ 2021

MASTER DEGREE THESIS
ON SPECIALITY
"AVIATION AND AEROSPACE TECHNOLOGIES "

Topic: "Boundary layer control system design for ultralight aircraft wing based on plasma actuators"

Fulfilled by: _____ **Valentyn MATVIIENKO**

Supervisor:
PhD, associate professor _____ Vad**i**m **ZAKIEV**

Labor protection advisor:
PhD, associate professor _____ **Victoria KOVALENKO**
Environmental protection adviser:
Dr. Sc., associate professor _____ **Tamara DUDAR**

Standards inspector
PhD, associate professor _____ **Sergiy KHIZNYAK**

Kyiv 2021

НАЦІОНАЛЬНИЙ АВІАЦІЙНИЙ УНІВЕРСИТЕТ

Аерокосмічний факультет
Кафедра конструкції літальних апаратів
Освітній ступінь «Магістр»
Спеціальність 134 «Авіаційна та ракетно-космічна техніка»
Освітньо-професійна програма «Обладнання повітряних суден»

ЗАТВЕРДЖУЮ
Завідувач кафедри, д.т.н, проф.
_____ Сергій ІГНАТОВИЧ
«_____» _____ 2021 р.

ЗАВДАННЯ

на виконання дипломної роботи студента

МАТВІЄНКА ВАЛЕНТИНА ОЛЕКСІЙОВИЧА

1. Тема роботи: «Розробка системи керування граничним шаром крила надлегкого літака на основі плазмових актуаторів», затверджена наказом ректора від 8 жовтня 2021 року № 2173/ст.
2. Термін виконання роботи: з 11 жовтня 2021 р. по 31 грудня 2021 р.
3. Вихідні дані до роботи: електросистема літака Piper Archer, конструкція крила Aeroprakt A20.
4. Зміст пояснювальної записки: аналіз систем керування граничним шаром крила літака, аналіз геометрії крила Аеропракт А20 та аеродинамічних профілей надлегких літаків, концептуальний проект блоку плазмогенератора, конструкція високовольтного імпульсного генератора, високовольтного інвертора змінного струму та спеціалізованих аеродинамічних мір.
5. Перелік обов’язкового графічного (ілюстративного) матеріалу: схеми блоку імпульсного високовольтного генератора, і інвертору, креслення загального вигляду аеродинамічних мір.

6. Календарний план-графік:

№	Завдання	Термін виконання	Відмітка про виконання
1	Огляд літератури за проблематикою роботи. Аналіз способів керування граничним шаром крила.	11.10.2021–13.10.2021	
2	Проведення аналізу аеродинамічних характеристик авіаційних профілей крила надлегких літаків.	14.10.2021–20.10.2021	
3	Розробка системи плазменного генератора для установки на надлегкий літак.	21.10.2021–24.10.2021	
4	Розробка обладнання для подальшого дослідження характеристик плазмових актуаторів.	25.10.2021–15.11.2021	
5	Виконання частин, присвячених охороні навколишнього середовища та охорони праці.	16.11.2021–21.11.2021	
6	Підготовка ілюстративного матеріалу, написання пояснювальної записки.	22.11.2021–29.11.2021	
7	Перевірка, редагування та виправлення пояснювальної записки.	30.11.2021–15.12.2021	

7. Консультанти з окремих розділів:

Розділ	Консультант	Дата, підпис	
		Завдання видав	Завдання прийняв
Охорона праці	к.біол.н., доцент Вікторія КОВАЛЕНКО		
Охорона навколишнього середовища	к.т.н, доцент Тамара ДУДАР		

8. Дата видачі завдання: 8 жовтня 2021 року

Керівник дипломної роботи _____ Вадим ЗАКІЄВ

Завдання прийняв до виконання _____ Валентин МАТВІЄНКО

NATIONAL AVIATION UNIVERSITY

Aerospace Faculty
Department of Aircraft Design
Educational Degree «Master»
Specialty 134 «Aviation and Aerospace Technologies»
Educational Professional Program «Aircraft Equipment»

APPROVED BY
Head of Department,
Dr. Sc., professor
_____ Sergiy IGNATOVYCH
«___» _____ 2021

TASK

for the master degree thesis

Valentyn MATVIIENKO

1. Topic: «Boundary layer control system design for ultralight aircraft wing based on plasma actuators», approved by the Rector's order № 2173/ст from 8 October 2021.
2. Period of work: since 11 October 2021 till 31 December 2021.
3. Initial data: electrical system Piper Archer aircraft, wing geometry of Aeroprakt A20.
4. Content: analyze of aircraft flow control systems, analyze of Aeroprakt A20 wing geometry and ultralight aircraft airfoils, conceptual design of plasma generator unit, designs of high voltage pulse generator, high voltage AC inverter and specialized aerodynamic scales.
5. Required material: schemes of high voltage pulse generator and invertor, drawings of the general view of aerodynamic scales.

6. Thesis schedule:

№	Task	Time limits	Done
1	Review of the literature on the issues of work. Analysis of the wing boundary layer control systems.	11.10.2021–13.10.2021	
2	Analysis of aerodynamic characteristics of airfoils for ultralight aircraft.	14.10.2021–20.10.2021	
3	Development of a plasma generator system for installation on an ultralight aircraft.	21.10.2021–24.10.2021	
4	Development of equipment for further study of the plasma actuators.	25.10.2021–15.11.2021	
5	Execution of the parts, devoted to environmental and labor protection.	16.11.2021–21.11.2021	
6	Preparation of illustrative material, writing the report.	22.11.2021–29.11.2021	
7	Explanatory note checking, editing and correction.	30.11.2021–15.12.2021	

7. Special chapter advisers:

Chapter	Adviser	Date, signature	
		Task issued	Task received
Labor protection	PhD, associate professor Victoria KOVALENKO		
Environmental protection	Dr. Sc., associate professor Tamara DUDAR		

8. Date of issue of the task: 8 October 2021 year

Supervisor: _____ Vadym ZAKIEV

Student: _____ Valentyn MATVIIENKO

РЕФЕРАТ

Пояснювальна записка дипломної роботи магістра «Розробка системи керування граничним шаром крила надлегкого літака на основі плазмових актуаторів»:

87 с., 49 рис., 3 табл., 24 джерел

Об'єкт дослідження – система керування граничним шаром.

Предмет дослідження – активна система керування граничним шаром для підвищення керованості та аеродинамічних характеристик при зльоті та посадці.

Мета магістерської роботи – розробка пристрою активного керування потоком літака для надлегких літаків для підвищення льотних характеристик.

Методи дослідження та розробки – аналіз працездатності пристроїв активного управління потоком літака з використанням експериментальних методів. Оптимізація аеродинамічних характеристик за допомогою ANSYS fluent і XFLR5. Програмне забезпечення SolidWorks використовувалось для моделювання та аналізу аеродинамічних мір.

Новизна результатів – розроблена нова конструкція системи керування граничним шаром крила надлегкого літака, розроблена нова конструкція аеродинамічних мір для досліджень плазмового приводу.

Практична цінність – розроблено, зібрано і протестовано обладнання для подальшого дослідження аєродинамічних характеристик плазмових актуаторів. Внесені пропозиції щодо покращення аеродинамічних характеристик надлегких літаків, на яких може бути встановлена активна система керування потоком без внесення значних змін в базову конструкцію.

МАГІСТЕРСЬКА РОБОТА, НАДЛЕГКИЙ ЛІТАК, ДІЕЛЕКТРИЧНИЙ БАР'ЄРНИЙ РОЗРЯД, АКТИВНЕ КЕРУВАННЯ ПОТОКОМ, ГЕНЕРАТОР ПЛАЗМИ, ПЛАЗМОВИЙ АКТУАТОР, ГРАНИЧНИЙ ШАР

ABSTRACT

Master degree thesis “Boundary layer control system design for ultralight aircraft wing based on plasma actuators”

87 p., 49 fig., 3 table, 24 references

Object of study – boundary layer control system design.

Subject of study – active boundary layer control system for increasing controllability and aerodynamic characteristics during take-off and landing.

Aim of master thesis – development of aircraft active flow control device for ultralight aircraft to increase flight performances.

Research and development methods – analysis of aircraft active flow control device performances using experimental methods. Optimization of aerodynamic performances using ANSYS fluent and XFLR5. SolidWorks software used for modeling and strength analysis of aerodynamic scales.

Novelty of the results – proposed new design of boundary layer control system for ultralight aircraft, designed a new aerodynamic scales for plasma actuator investigations.

Practical value – developed, assembled and tested equipment for further study of plasma actuators. Made suggestions to improve aerodynamic performances of ultralight aircraft on which active flow control system may be installed without making changes in the basic structure.

MASTER THESIS, ULTRALIGHT AIRCRAFT, DIELECTRIC BARRIER DISCHARGE, ACTIVE FLOW CONTROL, PLASMA GENERATOR, PLASMA ACTUATOR, BOUNDARY LAYER

CONTENT

ABBREVIATIONS

DBD – Dielectric Barier Discharge

SDBD – Single Dielectric Barrier Discharge

EMLA – Energy Methods of Lift Augmentation

BLC – Boundary Layer Control

MHD – Magnetohydrodynamics

MPA – Magnetoplasma aerodynamics

ADT – Aerodynamic tube (aerodynamic wind tunnel)

SEE – Single Encapsulated Electrode

MEE – Multiple Encapsulated Electrode

IC – Integrated Circuit

PCB – Printed Circuit Board

EMI – Electromagnetic Interference

AC – Alternative Current

DC – Direct Current

HV – High Voltage

IGBT – Insulated-gate Bipolar Transistor

MOSFET – Metal-oxide-semiconductor Field Effect Transistor

ADC – Analog to Digital Converter

MCU – Micro Controller Unit

PWM – Pulse-width Modulation

INTRODUCTION

Aircraft industry is one of the most technological industry of the world, it still faces many challenges. Every single manufacturer leads to increasing aerodynamic performances which determines the efficiency of the aircraft and its attractiveness for the target customer. Standard methods that involve changing of the aircraft geometry to achieve the required performances are well known, they force the designer to find compromise between maximum flight speed and speed of take-off and landing, between complexity of production, mass and final cost. Application of active flow control devices is one of the most promising areas for a radical improvement not only during takeoff and landing but also in cruise flight, maneuverability characteristics of aircraft for various purposes. Increasing the power-to-weight ratio and improving the aerodynamics of the aircraft due to the use of active flow control also makes it easier to solve the problem of reducing the noise level in the airport area due to the reduction of the required runway length and the use of steep climb trajectories during takeoff and descent during landing. The increased interest in these systems is due to the fact that their application makes it possible to solve problems that cannot be solved by conventional methods.

Alternative current (AC) and μs/ns pulse dielectric barrier discharge plasma actuators are one of the most promising technologies of active flow control and it's structure makes it's possible to install actuator system not only for new aircraft designs but also for existing ones. Unlike most active flow control systems, plasma actuator based system has high economic efficiency, low relative mass, which makes it suitable even for light unmanned aerial vehicles (UAV), and it has no moving parts. Fast responsiveness makes it possible to use them in active flight stabilization system, counter blades vibration and reduce noise emission.

The first part compares different types of active and passive flow control, describe its features and principle of work. Proposed a classification of flow control technics. There is a short look at the performances of subsonic flows that have been injected into electric and magnetic fields.

By the way plasma actuator can be incorporated into the design of existing aircraft's, it remains important to study the influence of aircraft geometric parameters on the efficiency of active flow control system. The second part considers effectiveness of high lift devices of ultralight aircraft on the example of Aeroprakt A20. The necessary calculation and simulations were carried out using ANSYS and XFLR5 software, which also show the points of flow separations and its transition to turbulent, this flow diagrames can be used to make conclusions about the optimal placement of the plasma actuators. Various airfoils were investigated, and the optimal airfoil is proposed for the operation in combination with active flow control system.

The third part is focused on integration of plasma generator in ultralight aircraft systems. The features of the plasma actuator operation are considered. The development of effective active flow control system will inevitably face the need for experimental research. The development of tools for the analysis of plasma actuators in experimental installations is an independent, valuable and urgent task. Special experimental equipment should be designed to test some components, prove efficiency and obtain some necessary experimental data. AC and ns/us pulse plasma generators schemes, were proposed, and investigated. Aerodynamic scales for work with plasma actuators is a complex structure which should take into consideration high electromagnetic interference (EMI) influence, provide good isolation for high voltage (HV) rails, etc. Such design were proposed, and assembled for further researches.

To perform experimental research in this field, an engineer needs a properly equipped laboratory or workplace, in accordance with state sanitary rules and regulations, which makes demands to many parameters, such as air ionization, requirements to high voltage equipment, ergonomic requirements for the organization of workplaces and workplaces. Harmful factors affecting a person in the process of performing experimental research will be considered. More details on this will be discussed in terms of labor protection.

The last part, environmental protection, is devoted to the problems of the negative impact of aviation on the environment and living organisms, as well as ways to solve these problems.

PART 1

ANALYSIS OF MODERN FLOW CONTROL METHODS

In order to improve the aerodynamic performance of the streamlined bodies, it is desirable to change the properties of their associated flows in a controlled manner over a range of conditions. In general, the methods developed to do so are called flow control methods. Flow control methods differ by their goals, physical mechanisms and technical implementation (Figure 1.1).

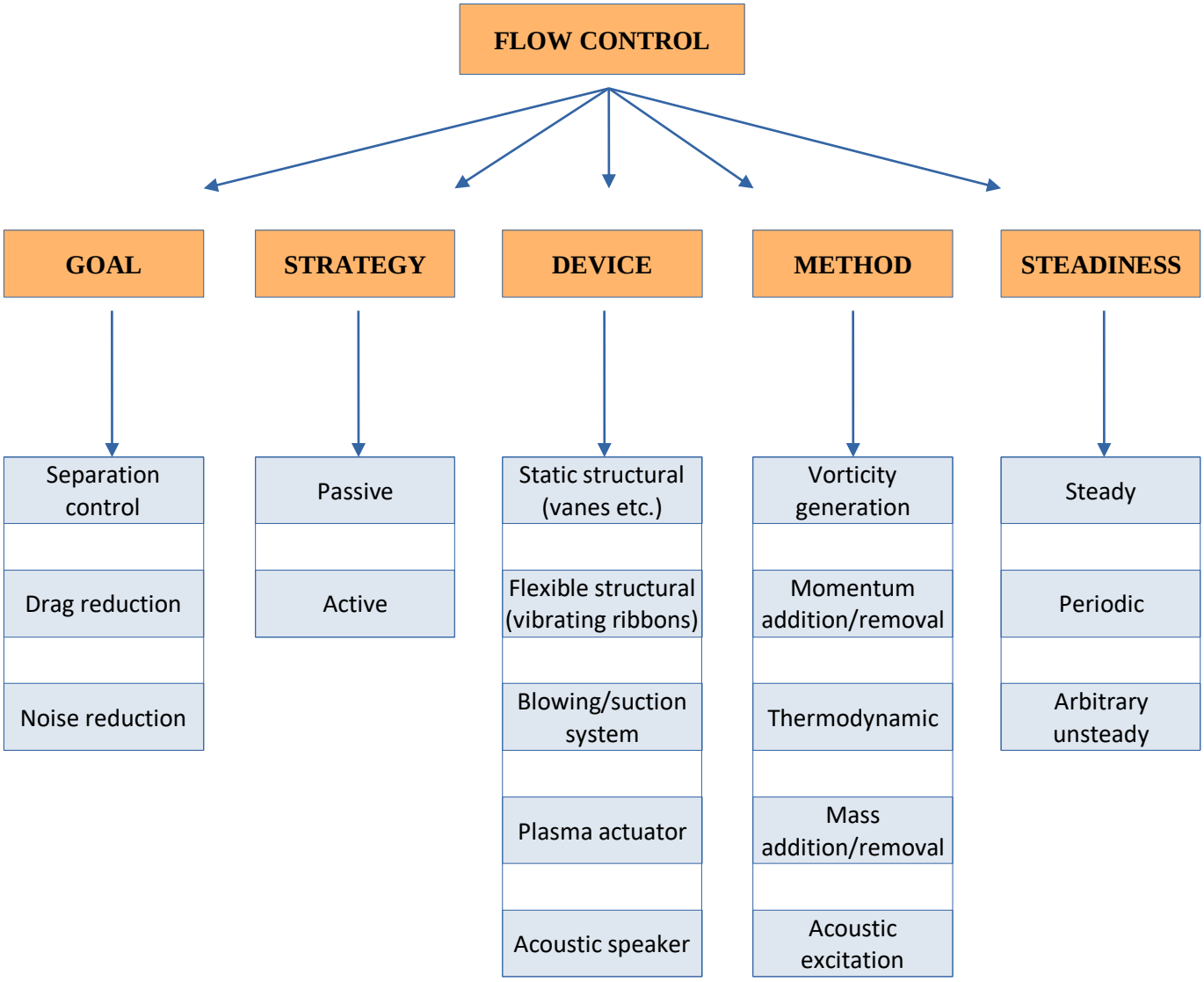

Figure 1.1 – Flow control methods classification

Goal defines strategies of design. Flow control device can be applied in order to increase lift or reduce drag and noise emission. Controlling separation of the airflow, both lift and drag can be controlled. Lift force also can be increased by controlling the circulation of the flow around an airfoil. Drag can be controlled by the moving of boundary layer transition points.

Strategy of flow control can be classified into passive and active. In comparison to active, passive strategies do not introduce additional motion into the flow, they are mostly structurally simple and have high reliability. However, the possibilities of these traditional passive methods are limited and are currently mostly exhausted. The action of the passive methods remains unchanged during the operation of the device and can work properly only in the optimal mode. Active methods, can vary its quantitative parameters (air consumption, energy, heat, etc.) according to the flow state obtained from sensors (pressure transducers, particle image velocimetry systems, hot wire velocity probes etc.), which creates possibility to adopt it for different flight conditions and allows adjusting to different turbulence regimes and operate equipment in a wide range of loads. Active methods subdivides into reactive and non-reactive.

Diverse devices can be used to interact with flow and change it's properties. They include static structural devices, usually installed on the surface of the aerodynamic object which are used for flow control (Ex. vanes, channels, ribbons, ramps, etc.). Flexible structural devices such as ribbon fairings can be used to suppress flow-induced vibrations. Another type of the device called actuator are designed specifically to bring additional types of motion into the flow. Such effects can be achieved by moving the parts of the object itself or by applying external forces to the flow medium (such as electric forces in plasma actuators). Blowing and suction devices also can be used to control flow on aerodynamic surface by adding or removal mass from flow, this in turn add or remove momentum, changing the velocity profile of boundary layers and other flow structures. Adding high-momentum fluid or removing low-momentum fluid makes velocity profiles fuller and helps boundary layers to overcome adverse pressure gradients, preventing separation and transition. Flow control can be classified by whenever they are steady or unsteady.

Research of active boundary layer control systems have been carried out at Central Aerohydrodynamic Institute (TsAGI) and other institutes for many years. In the 40s of the last century, one of the ways to improve the flow around the wing and flaps was the use of boundary layer suction through slots or perforations on the nose surface of the wing and on deflected flaps. In the early 50s, with the development of new jet engines, and the development of high-speed aircraft with thin wings, the main direction of research was the boundary layer and circulation control systems by blowing jets of compressed air taken from the jet engine onto the wing, flaps and control surfaces. The use of blowing jet increases the lift properties of the wing by restoring the continuous airflow at large angles of flaps deflection and large angles of attack, creating an additional load on the wing (supercirculation) and the vertical component of the deflected jet reaction. As a result of comprehensive studies of various types of Energy Methods of Lift Augmentation (EMLA) (Boundary Layer Control (BLC), jet flaps, etc.), a large amount of experimental material was accumulated, which was summarized in the Manual for Designers [1].

Further research was aimed at solving problems associated with the practical implementation of EMLA on aircraft for various purposes [2]. The effectiveness of the use of the BLC system on aircraft with wings of various shapes was investigated on transport aircraft An-10 [3] and An-42 [4] with straight wings, passenger aircraft with swept wings, maneuverable aircraft with variable geometry wings MiG-23 and with a trapezoidal wing MiG-25 [5]. On the basis of systematic research, the requirements for the parameters of the BLC systems were formulated, which ensure maximum aerodynamic efficiency at minimum energy costs, and the means for increasing the efficiency of the BLC were developed, the possibilities of increasing the efficiency of control bodies through the use of the BLC [3, 4] were developed and investigated. new means of longitudinal balancing of aircraft with highly effective types of take-off and landing wing mechanization was retractable front wings with slotted mechanization and BLC [6], a balancing circular cylinder with artificial circulation and others.

A comparative analysis of the effectiveness of boundary layer control systems by tangential blowing to the flaps and circulation control when blowing to the rounded trailing edge of the wing was carried out on the basis of the results of tests of the full-scale

experimental aircraft "Photon" in the T-101 ADT TsAGI. This aircraft was designed and manufactured according to the technical assignment of TsAGI at the Experimental student experimental aircraft design office of the Moscow Aviation Institute under the leadership of K.M. Zhidovetsky. Investigations of the aircraft, carried out in wide ranges of flap deflection angles $\delta_z = 0–180°$ and changes in the parameters of the blowing system to a rounded trailing edge, made it possible to obtain a unique material on the efficiency of these systems under conditions close to natural ones.

The results of researches of EBLCS are integrated in a number of collections of thematic articles and summarizing works. A review of early studies of energy systems for increasing lift is given in the book "Airfieldless Aviation" [7]. In the summarizing work [8], the analysis of the efficiency of using jet flaps and other circulation control systems was carried out. The results of a large number of researches of separated flows and various methods of flow separation control are summarized in the monograph [9]. The data of experimental and computational studies of circulation control systems by blowing onto a rounded trailing edge of a wing are given in a collection of articles published by the American Institute of Aeronautics and Astronautics (AIAA) [10]. General questions of the use of energy systems for short takeoff and landing aircraft are considered [11].

1.1 Example of flow control devices and it's comparison

Blowing. Blowing is one of the Energy Methods of Lift Augmentation (EMLA) certainly the most old and proven active flow control technology. It has already found application in many civil and military airplanes and has a strong theoretical base, which also may be used for research connected with another types flow control devices.

Potential for increasing the wing lift properties by increasing the curvature and angle of attack, determined by the calculation according to the theory of an ideal fluid, cannot be realized when using slotted mechanization. The main limitation of the possibilities of achieving the theoretical lift due to the use of slotted mechanization is the effect of viscosity and the occurrence of various types of flow separation on the wing. An effective method of preventing flow separation and increasing the lift is to blow jets of compressed air taken

from an aircraft engine or another autonomous sources from slot nozzles onto the upper surface of the wing or deflected flaps.

In order to study the features of the effect of tangential blowing of jets on the flow and aerodynamic characteristics of the wings TsAGI made research of a rectangular wing with an aspect ratio λ = 3 with a profile of large relative curvature and thickness (fmax ≈ 0.3, c = 0.15) (Fig. 1.2). The jets were blown out tangentially to the wing surface from slotted nozzles located on the nose, in the middle and in the tail airfoil part.

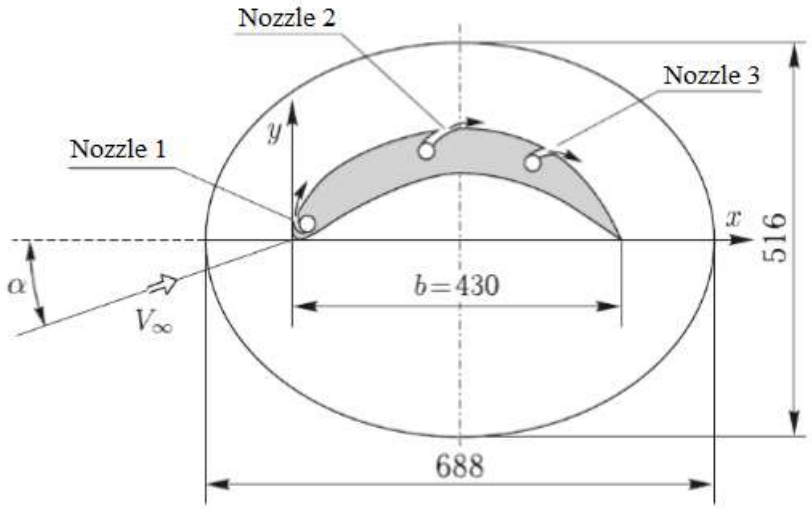

Figure 1.2 – Blowing on rectangular wing, location of nozzles

The intensity of jets was regulated by changing the compressed air pressure in the channels in front of the nozzles and was characterized by the value of the jet impulse coefficient:

$$C_\mu = \frac{m_c V_c}{q_\infty S} \tag{1.1}$$

where m_c is the second mass air flow rate, V_c is the jet outflow velocity, q_∞ is the incoming flow velocity head, S is the wing area.

Blowing leads to a weakening of the flow separation, decrease of pressure on the upper surface of the wing, and a more complete restoration of pressure on its lower surface (Fig. 1.3). At certain values of the momentum coefficient of the jet (C_μ = 0.07), the experimental pressure distribution turns out to be close to the theoretical one obtained according to the theory of an ideal fluid at C_μ = 0. This indicates the achievement of practically uninterrupted flow around the upper wing surface.

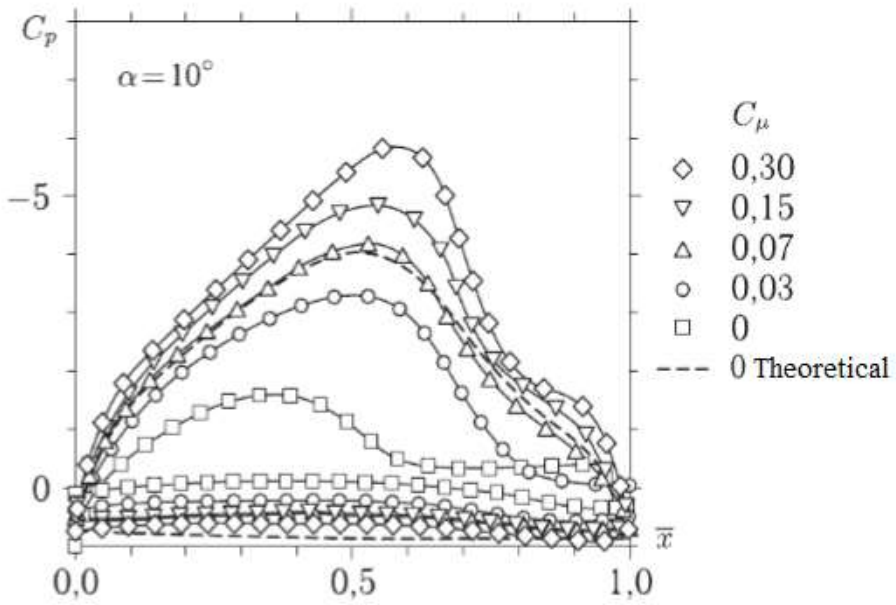

Figure 1.3 – Pressure distribution in the wing section with blowing from nozzle number 2

It has been calculated that when a disconnected separation occurs, the required air flow required for its elimination increases significantly.

Flight tests of the circulation control system efficiency were carried out on a light deck aircraft Grumman A-6A (Fig. 1.4) by tangentially blowing a jet onto a rounded trailing edge of the wing to improve takeoff and landing characteristics. A diagram of the modified A-6 CCW demonstrator aircraft with a wing circulation control system (CCW) is shown in Fig. 1.5. Compressed air for the TC system was discharged from the 12th stage with a flow rate of up to 10% of the total flow rate and a temperature of 338 ◦C. The width of the titanium slotted nozzle varies from 2.4 mm at the root to 1.2 mm at the end of the flap.

Figure 1.4 – Grumman A-6A aircraft

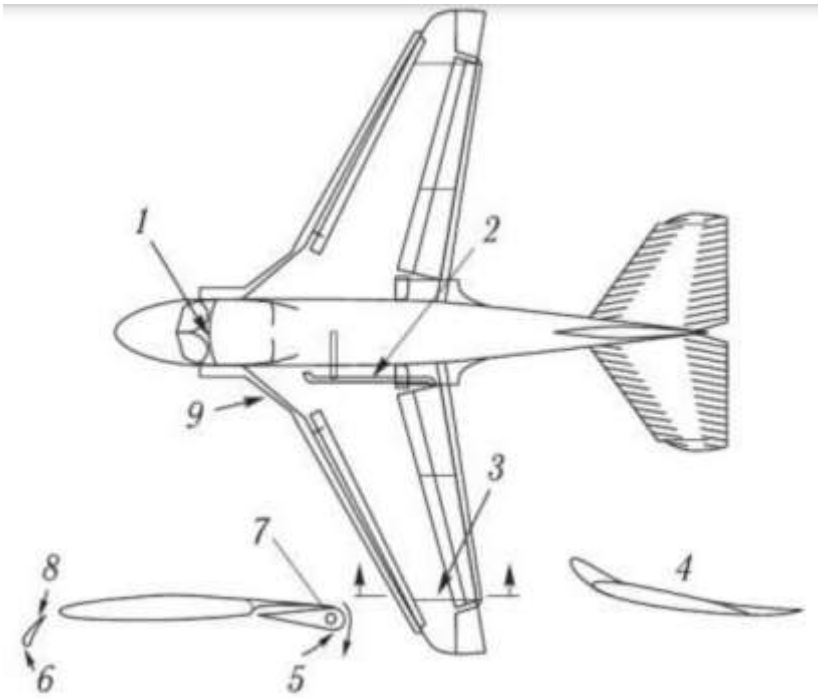

Figure 1.5 – Diagram of the A-6 CCW demonstrator aircraft with a wing circulation control system:

1 — CCW system controls; 2 — air ducts; 3 — ridge on the wing surface; 4 — modification of the stabilizer; 5 — rounded tail section of the wing; 6 — increased radius of the slat nose; 7 — pressure chamber and slot for air blowing out; 8 — slats fixed in position $\phi = 25^{\circ}$; 9 — additional Kruger flaps (in the extended position)

This tests shows that at optimal 60% of the maximum air flow rate in the circulation system the take-off speed of an aircraft with a take-off weight of G = 20.4 t decreases from $V_{take\text{-}off}$ = 212 km/h (aircraft without circulation system) to 174 km/h (18%), and the takeoff run decreases from L ≈ 580 m up to 400, that is, more than 30%.

Suction. Suction is one of the active flow control methods to prevent separation and delay transition. The idea of separation control via suction is to remove decelerated flow and thus deflect higher speed flow towards the surface (Fig. 1.6) .

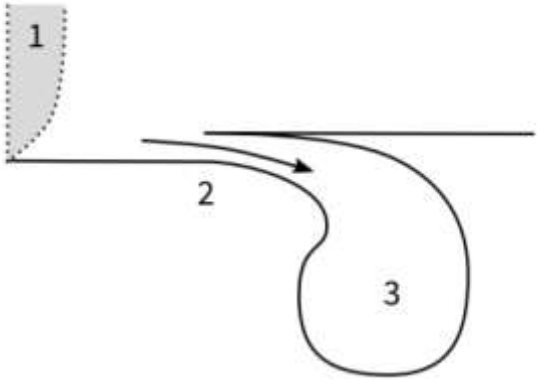

Figure 1.6 – Suction (removing low momentum flow from the boundary layer)
1 — incoming boundary layer profile; 2 — blowing/suction slit; 3 — internal plenum;

Suction is a promising direction for the radical improvement of the aerodynamic characteristics of the wings. An example of such system, is artificial flow laminarization by suction of the boundary layer on the nose of the wing, the study of which has been carried out for many years. However, the practical implementation of this system is associated with a number of technological, design and operational problems (laboriousness of manufacturing a perforated surface with a large number of micro-holes, large required internal channels for suction of low-pressure air, power take-off from the power plant to drive the suction units, the problem of contamination and icing of the perforated surface , as well as its strength, resource, etc.).

Surface motion. Surface motion Another method for boundary layer control is surface motion. Generally it involves the parts of the model moving with approximately the same velocity as freestream flow, thus eliminating the boundary layer. Examples of this

technique include rotating cylinders on leading (Fig. 1.7) and trailing edges, and moving floors in wind tunnels for car aerodynamic measurements.

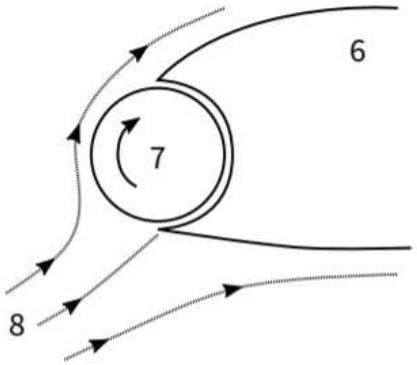

Figure 1.7 – Rotating leading edge system

6 — wing; 7 — rotating cylinder; 8 — incoming freestream

Combined systems. Such systems more that one flow control systems to increase it's efficiency. An example of such system is the ejector flap (Fig. 1.8) provides an increase in the lift properties by controlling the boundary layer by sucking (ejecting) air from the wing and flap surfaces, increasing the velocity circulation when the jet is blown out of the wing, as well as increasing the available impulse of the jet in the mixing chamber of the ejector, formed by the flap elements, in comparison with the impulse of the active jet in the ejector. An increase in the lifting force of the wings with the control center occurs both due to the effect on the flow around (aerodynamic effect) and due to the vertical reaction of the blown jet.

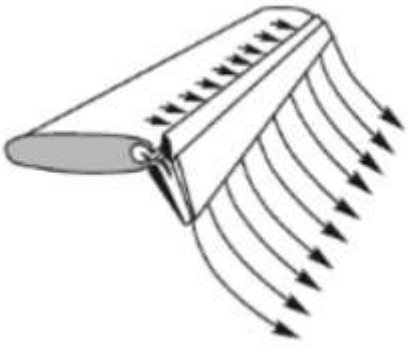

Figure 1.8 – Ejector flap

Acoustic excitation. Using sufficient acoustic excitation, it is possible to excite Tollmien-Schlichting (TS) instability waves within a boundary layer. This delays separation, since turbulent boundary layers are less susceptible to separation than laminar ones. The effectiveness of acoustic excitation has been demonstrated on the large variety of airfoils from flat plates to 17% thick airfoils, reaching a maximum of 40% lift coefficient increase (but not in CLmax) [23].

Plasma flow control. Since the 1950s, magnetohydrodynamic (MHD) interaction has attracted great interest from an aerodynamic point of view. The first studies were aimed at elucidating the fundamental aspects of the influence of the magnetic field on the characteristics of hypersonic flows of ionized gas around various bodies [12, 13]. The main aerodynamic effects initiated by the magnetic field were established.

Interest in the use of weakly ionized plasma in aerodynamics began to form in the early 1980s. Then, in the first works [14] on the passage of shock waves through a weakly ionized gas, the effects of an increase in the wave velocity, broadening of the front, and a number of others were noted. In most cases, the effect of a weakly ionized plasma on the flow is manifested in the release of energy from the currents flowing through the discharge region. From the point of view of mechanics, the effect of the thermal mechanism on the flow characteristics can be considered as fundamentally studied [15, 16].

To the nonthermal mechanisms, great interest has the processes of charge separation in the front of a shock wave [17], arising during the passage of a wave through a plasma. Potentially, the space charge layers affect the structure of the wave front (and the flow as a whole) due to the appearance of an electrostatic force. Recently, studies of the possibility of flow control using electrostatic force have attracted great interest.

First researches were conducted by using direct current (DC) corona discharge principle. Main disadvantages of these actuators are low flexibility in electrodes configuration and in the supply system, and the transition into spark regime producing irreversible damage of the actuator itself.

Recently a new active flow control technique has been investigated that has the potential to achieve significant increasing of aerodynamic performances, namely, the single dielectric barrier discharge (SDBD) plasma actuator. These have been extensively studied

over the last decade. One of the first patents, which used DBD for changing of aerodynamic performances was RU №2492367. The method is used for laminarizing of the boundary layer on an aerodynamic surface, for example a wing, is implemented using a device (Fig. 1.1) containing a dielectric section of surface 2 on the wing 1, with a system of cells 3 (Fig. 1.2), each of which consists of a pair of electrodes: an open linear plate electrode 4, located on surface 2 flush, and a closed electrode 5 located under surface 2, connected to a source 6 of high voltage alternating current, and the electrodes 4, 5 in each cell 3 are oriented parallel to the leading edge 7 of the wing, the closed electrode 5 is offset relative to open electrode 4, towards the tail part 8 of the wing, a hot-wire anemometer sensor 9 for measuring velocity pulsations in the boundary layer.

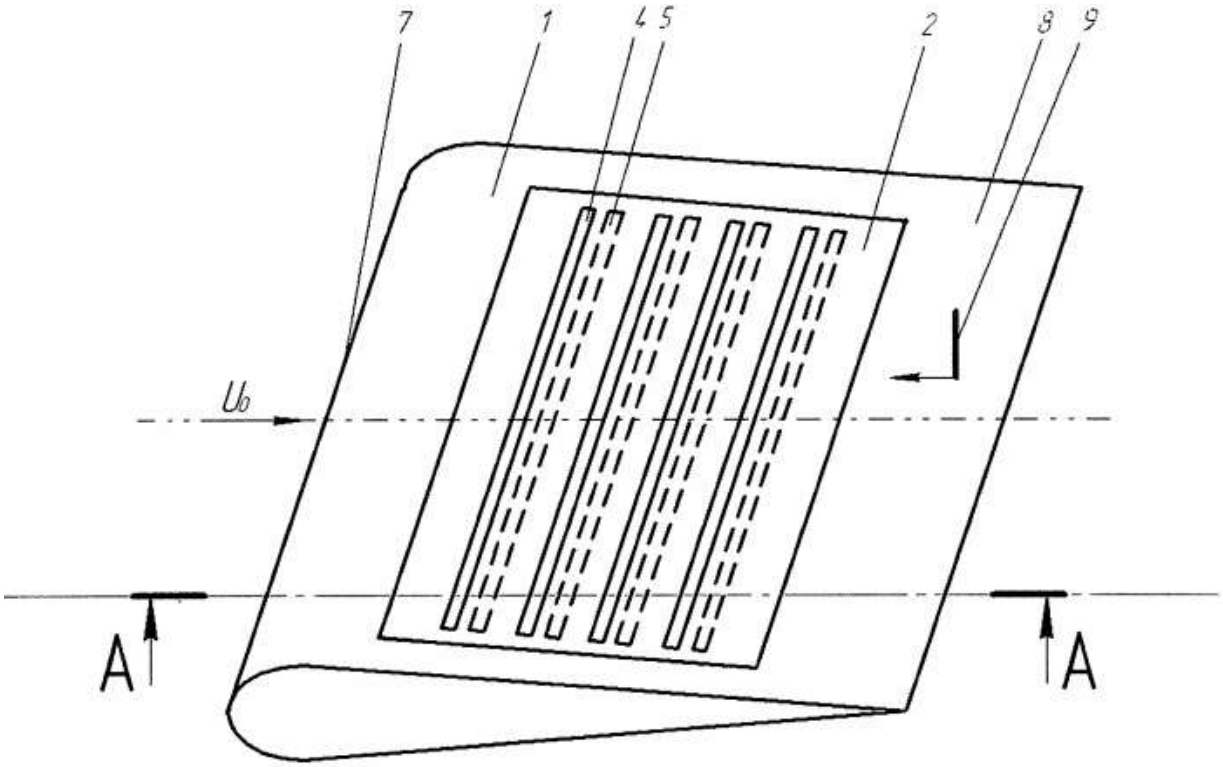

Figure 1.9 – Device for laminarizing of boundary layer

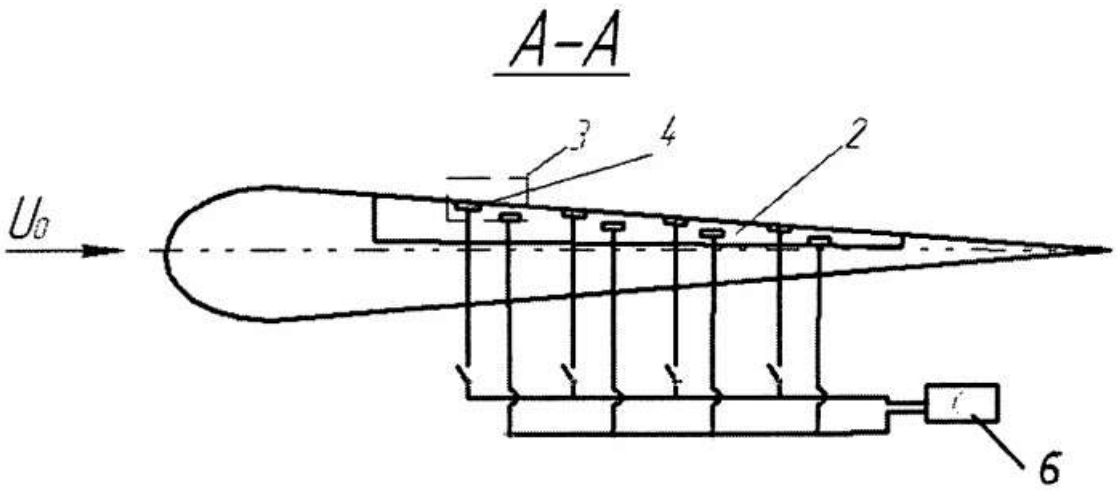

Figure 1.10 – Device for laminarizing of boundary layer (Side view)

The presence of the plasma and the particular electrode configuration induce a jet tangential to the actuator wall, similar to a classic blowing technique that was described earlier[2]. These jets can modify the aerodynamic boundary layer, increasing flow momentum, at least in the near-wall region above the surface.

1.2 Alternative current dielectric barrier discharge actuator

Typical single dielectric barrier discharge (SDBD) actuator system consists of two electrodes separated by a dielectric layer (kapton, plastics, fiberglass, quartz, ceramics, etc). Electrodes can overlap, or the edges of the electrodes can coincide, or there can be a gap between electrodes. The encapsulated electrode is connected to the ground and the exposed electrode is connected to a high voltage AC power supply. Required voltage for AC actuator are in the kV range and applied with a frequency in the kHz range (typicaly 5-20kHz). During operation, a blue-violet plasma glow is visible, originating at the edge of exposed electrode and spreading out across the dielectric surface that is above the encapsulated electrode as shown in Fig. 1.11, this length depends on applied voltage, thickness of dielectric layer and geometrical parameters of encapsulated electrode. Discharge appears to be macroscopically homogeneous to the unaided eye, but it is constituted by a sequence of micro-discharges lasting typically for tens of nanoseconds with a repetition rate of several hundreds of megahertz. Fast ignition and quenching of the discharge can be inferred by voltage-current time behavior reported in Figure 1.12. The speed of ionic wind are mostly

depends on applied frequency and voltage amplitude. Speed is decreasing with increasing of frequency also Joule heating becomes much more noticeable.

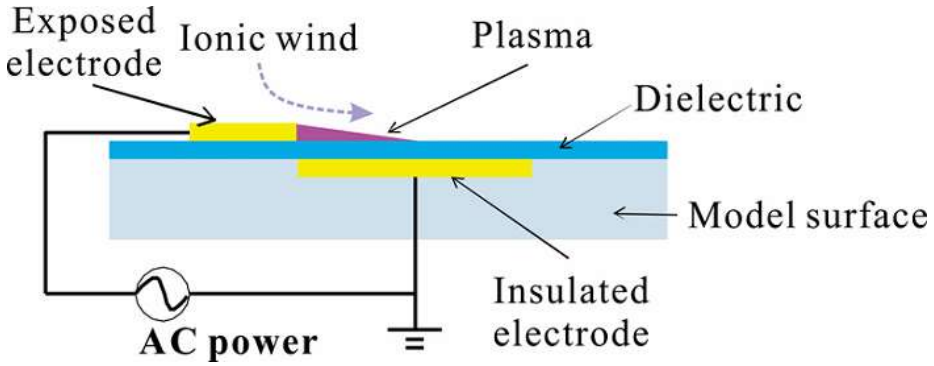

Figure 1.11 – Standard dielectric barrier discharge plasma actuator configuration.

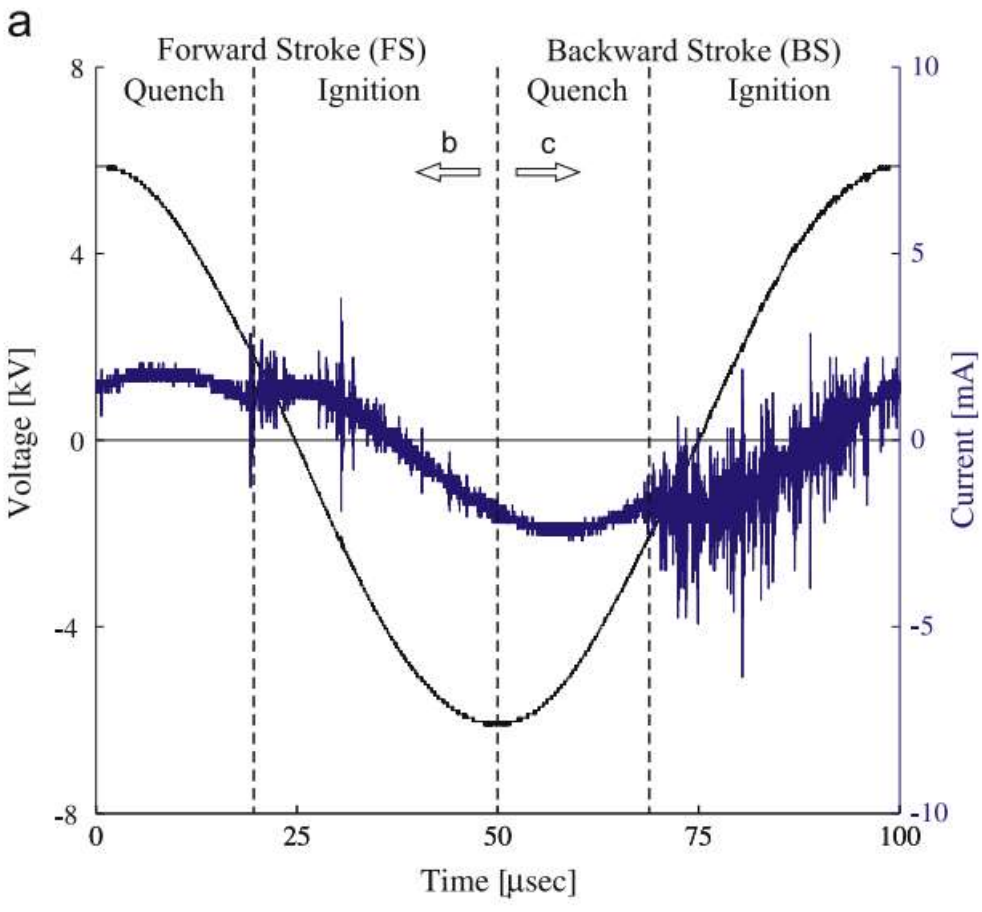

Figure 1.12 – Voltage-current time behavior of a SDBD

The plasma is ionised air consisting of ions and electrons with the bulk plasma exhibiting electrical neutrality. The remarkable aspect of this arrangement is that it has the

ability to produce a steady jet that flows away from the exposed electrode across the encapsulated electrode on the scale of seconds, without the need for any moving parts.

The force f per unit volume within the discharge can be yield by the following expression:

$$f = (n_i - n_c)\overline{E} \tag{1.2}$$

where $\overline{E}$ is the electric filed and n_i and n_e are ion and electron number density respectively.

The plasma actuator is lightweight, easy to repair, flexible and able to follow the curvature of the surface it is applied to. It can be switched on or off or passive at the flick of a switch, can be activated at a wide range of modulation frequencies and has a high frequency response. The entire system is all-electric and fits in well with the current ethos of aircraft manufacturers to produce all electric aircraft's.

The efficiency of the AC actuators can be measured as a ratio of the mechanical power, given by Eq. (1.2), to the electrical power.

$$Power_{mech} = \int_0^\infty \frac{1}{2}\rho v(Y)^3 l dY \tag{1.3}$$

where ρ is the air density, v(Y) is the velocity profile and l is the electrode length.

The efficiency DBD AC of the plasma actuator at imparting mechanical power into the flow is low, 0.05% maximum in the cases tested. Actuators with plasma lasting for longer portions of the cycle do not always produce higher velocity induced jets. μs-DBD and ns-DBD can have much more efficiency due to another principle of work.

1.3 Pulse dielectric barrier discharge actuator

As mentioned earlier, high influence on actuator performance has voltage waveform, amplitude and frequency. When the high-voltage profile is sinusoidal (AC-DBD), the charged particles in the plasma move under the action of the electric field force, inducing an ion wind with the velocity less than 10 m/s. When the high-voltage profile is pulsed with microsecond/nanosecond time scale (μs-DBD/ns-DBD), the ion wind velocity is lower than 1 m/s, but a fast generation of Joule heat will be observed, which can produce strong disturbance in the flow field and suppress the boundary layer separation. The effective free-stream velocity range of μs-DBD/ns-DBD (0.8 Ma) is much larger than that of AC-DBD (0.4 Ma) because of the limited velocity of the ion wind induced by AC-DBD. There are

many research studies using a DBD plasma actuator for wing flow control in recent years. Applied frequency to ns-DBD actuator has a great influence and can improve the aerodynamic performance of the flying wing at different Reynolds numbers. The results show that there is an optimal actuation frequency, which better delays the rupture of the leading edge vortex [23]. Most of the studies are carried out with small models and comparatively high free-stream velocity, making the test Reynolds number around 10^5. However, the target condition (taking off and landing) of the plasma flow control is mainly at a relatively low speed and high Reynolds number, which means a large scale experimental model and a large wind tunnel. Whether the DBD plasma actuation is still effective in high Reynolds number ($>10^6$), relatively lower speed (<0.3 M), and complex wing profile. Therefore, it is necessary to research the plasma flow control with a large scale complex profile at a high Reynolds number for engineering applications.

Many studies have been conducted to optimize the plasma actuator in an attempt to improve performance [18, 19]. Variables that influence plasma distribution and intensity are voltage waveform, voltage amplitude, frequency, electrode configurations, background gas, dielectric material, dielectric thickness and dielectric temperature [20, 21]. Optimization of the plasma actuator has shown the importance of the supplied signal as well as the geometry of the electrodes. Correct material selection, especially for the dielectric layer, can lead to large performance gains most notably from the reduction of dielectric heating [22].

It was found that the flow control effects of the DBD plasma actuator are closely linked with the relationship between the pulse frequency and the inherent frequency of the flow field. When these two frequencies are well coupled (with the reduced frequency $F^+=f\cdot C/v=$ 1), good flow control effects can be obtained on the airfoil[12]. Therefore, experiments need to be conducted with different pulse frequencies to verify this rule of frequency on the flying wing model at a high Reynolds number and finally to find the optimum pulse frequency.

Fig. 1.13 and Fig. 1.14 show the enhancement of the aerodynamic performance in the experimental setup with different pulse frequencies at the flying wing with Reynolds number of 1.86×10^6. The plasma actuator with the actuation voltage of 10 kV is mounted full span-wise at the leading edge. It can be seen from the curves that the best flow control

performance appears when the pulse frequency is in the range of 50–300 Hz. When the pulse frequency is 100 Hz, the lift coefficient enhancement is maximized. When the pulse frequency is higher than 300 Hz, the flow control effect becomes relatively poor.

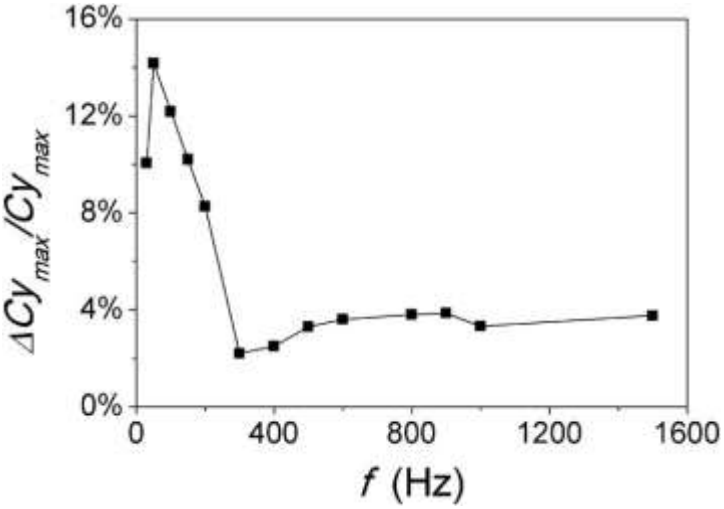

Figure 1.13 – Lift coefficient variation with different pulse frequency.

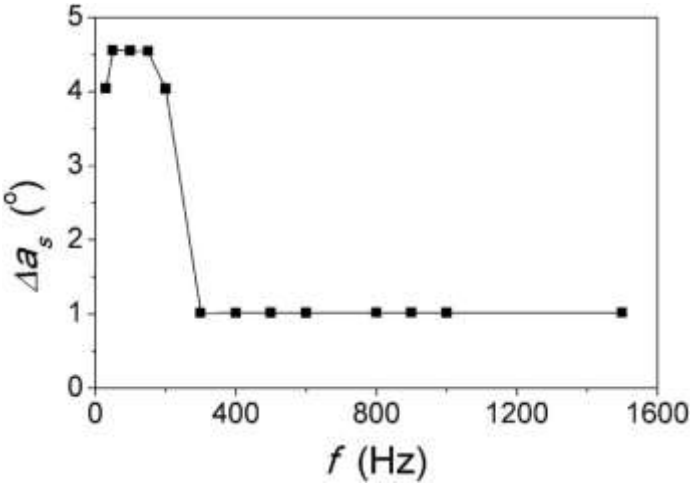

Figure 1.14 – Stalling angle enhancement with different pulse frequencies.

1.4 Dielectric barrier discharge plasma actuator types

Among the many existing plasma actuator designs, it is possible to distinguish two main types: baseline plasma actuator and multiple encapsulated electrode (MEE) plasma actuator.

The single encapsulated electrode (SEE) actuator (Fig. 1.11) consists of an exposed electrode constructed from thick tinned copper foils. The encapsulated electrode is

constructed from the same material but with a higher wide. Kapton tape can be used as dielectric and layered on top of the encapsulated electrode. The actuator can be mounted on a Perspex substrate and there is no offset between the edges of successive electrodes.

In article “Development of DBD plasma actuators: The double encapsulated electrode” [24] was proposed next design for SEE actuator: exposed electrode constructed from 74 μm thick tinned copper foils, 5 mm wide and 100 in length, encapsulated electrod constructed from 74 μm thick tinned copper foils, 50 mm wide with the same length, devided by kapton tape with 540 μm thickness.

Multiple encapsulated electrode (MEE) plasma actuator (Fig. 1.15). It has multiple encapsulated electrodes that are distributed throughout the dielectric layer. The maximum depth, overall width and polarity of the encapsulated electrode remains the same as in SEE throughout all configurations.

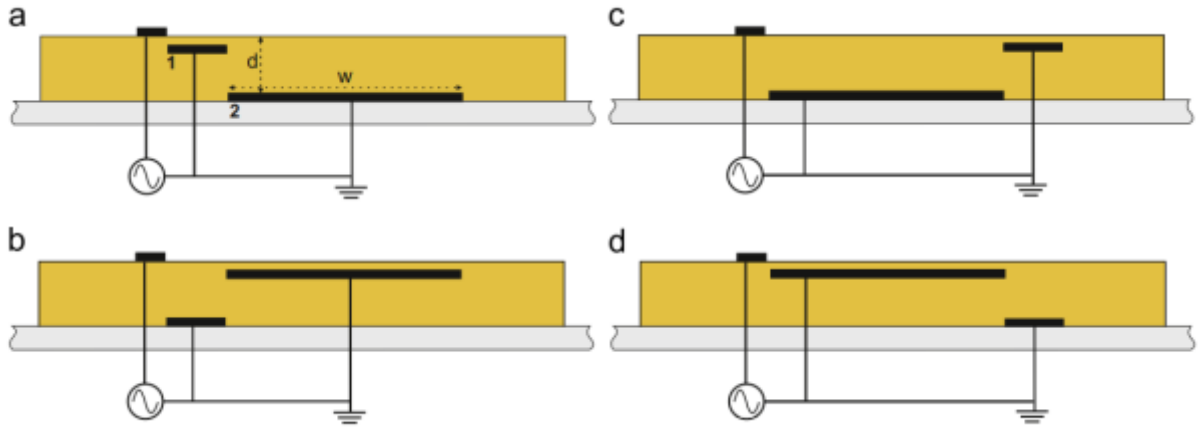

Figure 1.15 – Multiple encapsulated electrode plasma actuator configurations.

Manipulation of the encapsulated electrode has been shown to alter the performance of the dielectric barrier discharge plasma actuator. Locating the initial encapsulated electrode closer to the dielectric surface results in a earlier plasma ignition time and the plasma discharge being present for longer in the discharge cycle. This is the same result found when increasing the applied voltage to the baseline actuator. Manipulation of the encapsulated electrode to locations closer to the dielectric surface results in induced velocities higher than the baseline case for a given voltage. For the double MEE cases the maximum induced velocity was 91.2% higher than the baseline case for a 26.2% increase in power consumption. Actuators with a deep initial electrode are able to induce higher

velocities at lower power consumption than the standard actuator. Actuators with shallow initial electrodes use more power than the baseline case at a given voltage. Conversely, actuators with a deep initial electrode use less power than the baseline case at a given voltage.

Conclusion to the Part 1

Implementation of active flow control system on an aircraft is a complex task that includes the problems of aerodynamics, structure design and, finally, the choice of a rational aerodynamic scheme and layout of the aircraft. The comparative analysis of these systems made it possible to draw the main general conclusions about the advantages and disadvantages of each system (Table 1.1).

Table 1.1 – Active flow control comparison

	Advantages	Disadvantages
Blowing	- high aerodynamic efficiency. For example, blowing onto simple rotary non-slotted flaps at with optimal impulse ensures their uninterrupted flow and an increase in efficiency by 2.5–3 times and 1.5–2 times compared to the efficiency of slotted flaps when they are deflected at large angles. Blowing from the leading edge of the wing to its upper surface increases the maximum lift force and the critical angle of attack by 25–30% at the blowing intensity C_μ = 0.03–0.05; - ease of operation (slotted nozzles are automatically cleaned of dirt and icing formation when the compressed air or gas supply system is turned on); - relatively small values of the momentum coefficient of the blown jets required to achieve a continuous flow around the flaps and the upper wing surface at high angles of attack; - flight safety. In the case of system failure, aircraft can continue safety operation.	- technological complexity with manufacturing of narrow slotted nozzles (h_s □ 0.2–0.5mm); - complicated design increase mass of the aircraft due to equipping with a compressed air (hot gas) system which also decrease engine thrust; - very complicated for small aircraft which haven't air jet engines with multiple compressor stages;
Suction	- significant increasing of lift coefficient (even more in comparison to blowing) due to the combined aerodynamic effects of suction of the boundary layer from the wing and supercirculation;	- complicated structure and high mass; - significant decreasing of effectiveness with the increasing of flight speed;
Surface motion	- increasing of lift coefficient and drag decreasing due to elimination of the boundary layer;	- increase mass of the aircraft; - in most cases can not care high loads;

		- difficult to apply in real aircraft, due to deformation of wing during flight;
Acoustic excitation	- delays separation, from which lift coefficient can be increased up to 40%. - can decrease noise emission;	- inefficient on high angles of attack;
AC DBD plasma actuator	- increase maximum angle of attack and lift coefficient up to 30%; - can be used for laminarization of boundary layer across upper surface; - design simplicity, and low mass of system, which makes possibilities to apply it on light aircraft's and small UAVs; - No moving parts - Controllability and fast response	- inefficient on high Reynolds numbers and flight speeds; - requires high voltage power supply;
us/ns impulse DBD plasma actuator	- increase maximum angle of attack and lift coefficient up to 30%; - due to another physical principle of influence on flow, can be applied even in high Reynolds number and flight speed; - lower power consumption in comparison to AC actuators.; - design simplicity, and low mass of system, which makes possibilities to apply it on light aircraft's and small UAVs; - No moving parts - Controllability and fast response	- requires high voltage power supply; - due to short rise and fall time, electromagnetic influence on another aircraft systems should be considered;
DC corona discharge actuator	- very simple in design - influence on the boundary layer is similar to AC DBD actuator. - No moving parts - Controllability and fast response	- requires high voltage power supply; - can’t be operated when surface between electrodes contaminated or wet (only with good weather conditions); - electrodes can be easily damaged if corona discharge transfers into sparc discharge.

PART 2
ANALYSIS OF ULTRALIGHT AIRCRAFT AS A BASE FOR PLASMA ACTUATOR APPLICATION

This work is carried out in connection with the increasing demand for light aircrafts which can be operated on short runway. The purpose of this work is to determine the optimal location of plasma actuators and it's system units, create suggestions for improvement of wing geometry and structure to advance flight performances, taking into account the usage of active flow control device.

2.1 Overview general performances

One of the main priority to the plane is the simplicity of design in combination with good aerodynamic properties. For this purpose, aircraft based on Aeroprakt A20 was selected. The A-20 fuselage is constructed with three layers sandwich panels, metal consoles, covered by aircraft polymer fabric or 2024T3 aluminum (depending on region modification) and composite tail. The wings fitted with full-span flaperons, to increase total lift during take-off and land. Wing consoles cross section is good proven R-III airfoil with 15.5% thickness. Flap control in three fixed positions: 0 degrees, 20 degrees and 30 degrees, they are quite effective and decrease the landing speed up to 30 mph (48 km/h). The disadvantages of the upper location of the wing include a decrease in the efficiency of vertical stabilizer at high angles of attack, when the stabilizer enters at turbulent stream from the wing, in this case plasma actuators also can be considered to increase efficiency of stabilizers. The conventional landing gear has steel sprung main gear legs.

The A-20 was originally designed for the 50 hp (37 kW) Rotax 503 two- stroke aircraft engine. The low drag airframe produces acceptable performance on this low power output. Optional engines include the 64 hp (48 kW) Rotax 582 and 100 hp (75 kW) Rotax 912ULS.

General view of A20 prototype are presented in Fig. 2.1 and it's performances are presented in table 2.1.

Table 2.1 – Aeroprakt A20 performances

PARAMETER	VALUE
Maximum speed, km/h	140
Stall speed, km/h	46 km/h
Maximum flight range (fuel 38L, no wind), km/h	400 km
Maximum flight time, hours	4.5 h
Climb rate, m/s	3 m/s
Minimum rate of decline, m/s	1.8 m/s
Take off distance, m	80 m
Wingspan, m	11.4 m
Length, m	6.7 m
Height, m	1.8 m
Wing area, m^2	15.7 m^2
Maximum take-off weight, kg	450 kg
Empty weight, kg	218 kg
Overload	+4/-2

Fig. 1.3 – Aeroprakt A20

2.2 Aeropract A20 Wing geometry analysis

As mentioned earlier, the wing of the aircraft based on R-III-15.5 airfoil, consists of a center section, two detachable consoles, and a system of struts. The wing consoles are connected to the fuselage by torque-less nodes and a strut system. The wing is equipped with slotted flaperons.

Wing cross section is shown on Fig. 2.2. Between main console and flaperon present a gap in any position. A stream of air from bottom part of the wing passes through it, directed into the low pressure zone formed above the wing of the aircraft. This flow prevents early flow stalling.

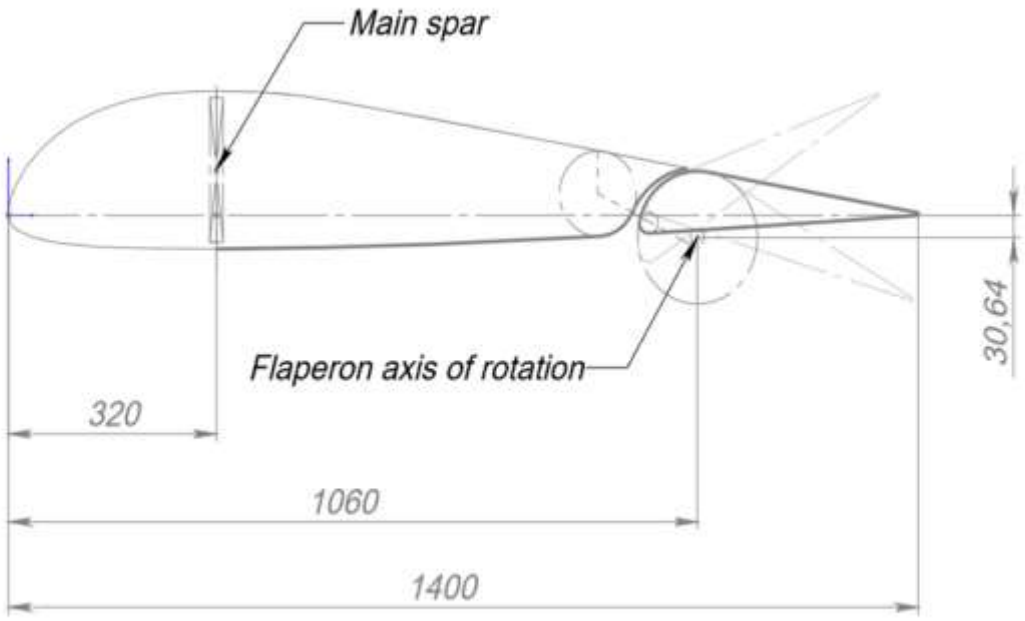

Fig. 2.2 – Wing cross-section geometry

To verify effectiveness of such geometry, some numerical calculations and simulations were carried out. For analysis ANSYS 2019r2 were used, mesh is shown on Fig. 2.3, flow velocity for all tests is equal 20m/s, turbulence model k-omega, flow is laminar, number of iterations 2000 or less if full convergence were reached (in all cases).

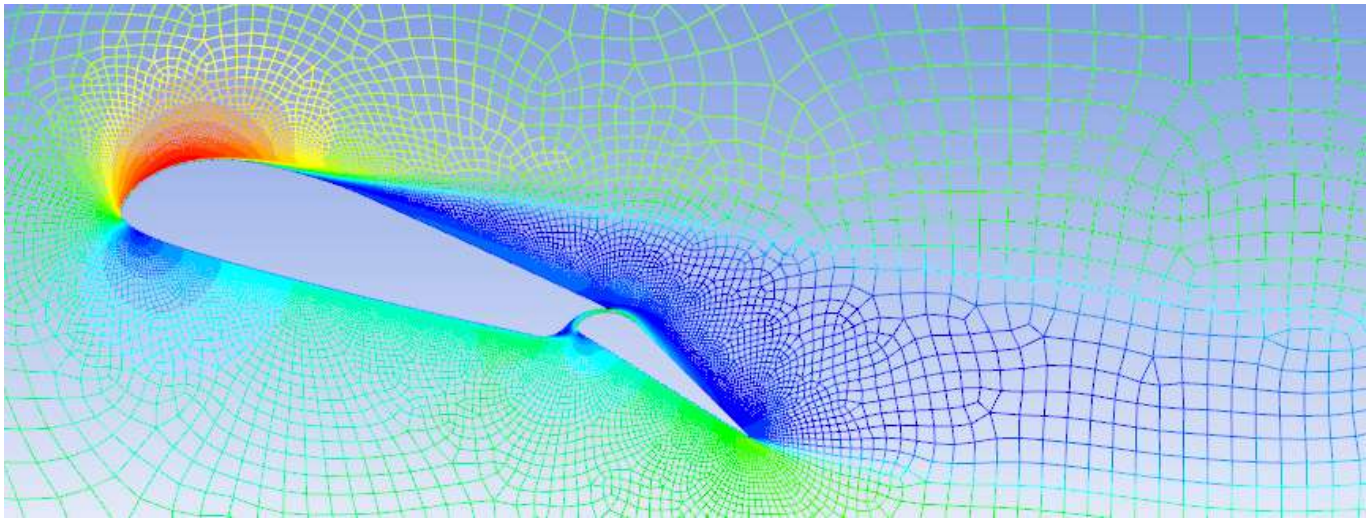

Fig. 2.3 – Mesh for ANSYS simulation.

Maximum angle of attack for R-III 15.5 is equal ~18°, but for safety operations it restricted to 15°.

Input data for simulations:

Simulation 1.0:

- Angle of attack $\alpha = 15°$;
- No flaps;
- Speed $V = 20$m/s;
- Density $\rho = 1.225$;
- Reynolds number $V \bullet b \bullet 70000 = 20 \times 1.4 \times 70000 = 1960000$

Simulation 1.1:

- Angle of attack $\alpha = 15°$;
- Angle of flap in relation to the wing $\alpha_{flap} = 0°$;
- Speed $V = 20$m/s;
- Density $\rho = 1.225$;
- Reynolds number $V \bullet b \bullet 70000 = 20 \times 1.4 \times 70000 = 1960000$

Simulation 1.2:

- Angle of attack $\alpha = 15°$;

- Angle of flap in relation to the wing $\alpha_{flap} = 20°$;
- Speed $V = 20$m/s;
- Density $\rho = 1.225$;
- Reynolds number $V \bullet b \bullet 70000 = 20 \times 1.4 \times 70000 = 1960000$

Simulation results should be corrected in accordance with experimental data and wing chord length (in CFX analysis, chord length equal 1.4m, that is why C_Y has greater value):

$$c_y\ (\alpha = 15,\ \alpha_{flap} = 0)\ (b = 1.4) = 1.0844\text{e-}01 + 2.1858\text{e+}00 = 2.294$$

$$c_y\ (\alpha = 15,\ \alpha_{flap} = 0)\ (b = 1) = c_y\ (b = 1.4)\ /1.4 = 1.638$$

$$c_y\ (\alpha = 15,\ \alpha_{flap} = 20)\ (b = 1.4) = 2.9019\text{e-}01 + 3.3222\text{e+}00 = 3.61$$

$$c_y\ (\alpha = 15,\ \alpha_{flap} = 20)\ (b = 1) = c_y\ (b = 1.4)\ /1.4 = 2.579$$

Correction coefficient $k_{y\ correction} = C_{y\ actual} / c_y\ (b = 1) = 1.42/1.638 = 0.867$, than:

$$C_y\ (\alpha = 15,\ \alpha_{flap} = 0) = 0.867 \bullet 1.638 = 1.42$$

$$C_y\ (\alpha = 15,\ \alpha_{flap} = 20) = 0.867 \bullet 2.579 = 2.24$$

Velocity distribution diagram for simulation 1.2 is shown on Fig. 2.4 and turbulence kinetic energy on Fig. 2.5.

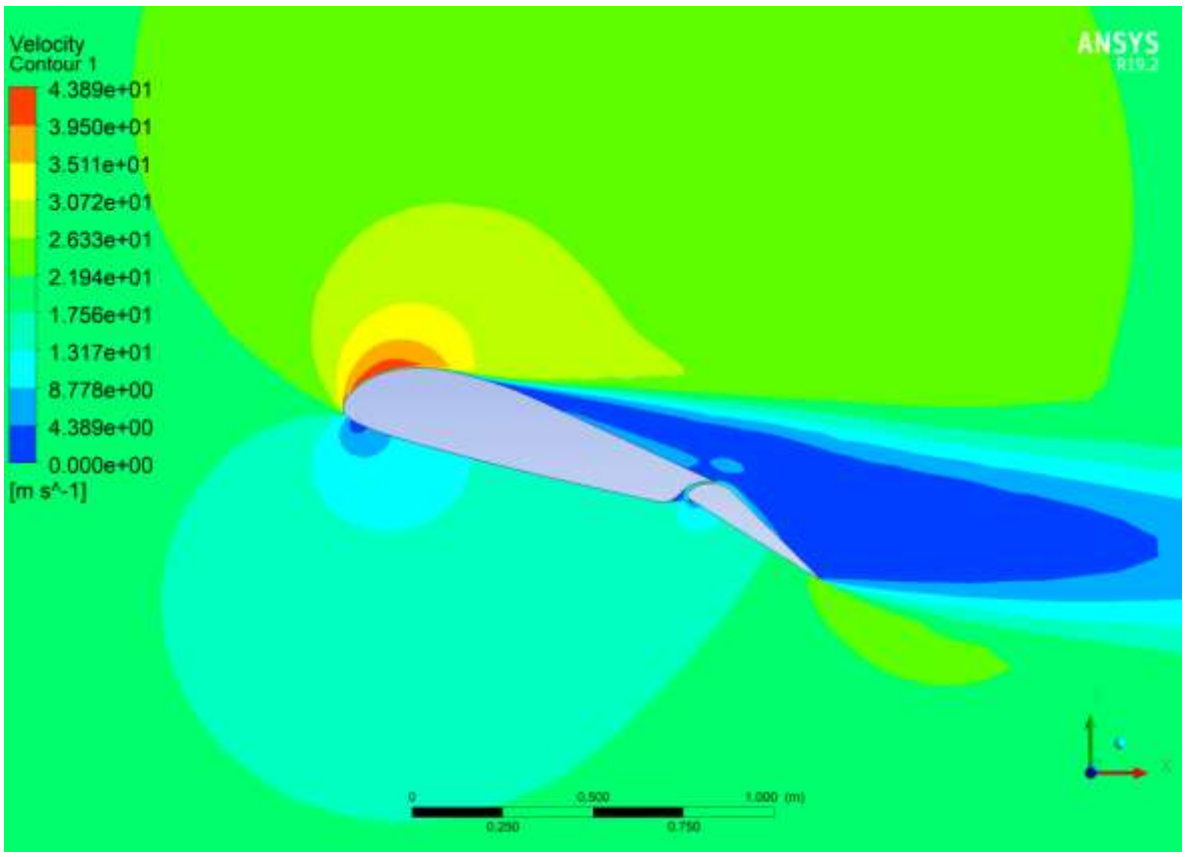

Fig. 2.4 – Velocity diagram.

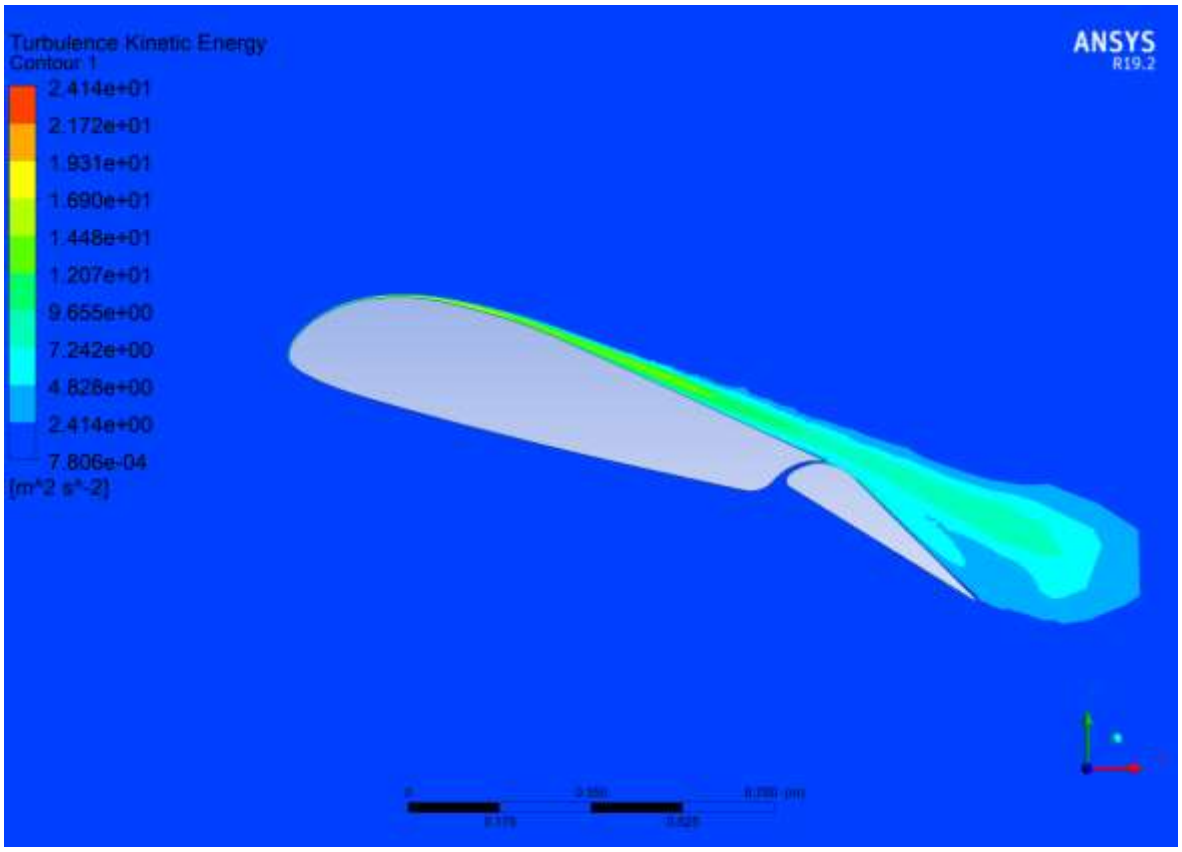

Fig. 2.5 – Turbulence kinetic energy diagram.

Wing geometry of Aeroprakt A20 was analyzed by fulfillment of ANSYS simulations which showed transition points, which can be used to define location of plasma actuators.

2.3 Modification of wing cross-section for ultralight aircraft

To increase efficiency of aircraft, in this subpart will be considered alternative airfoils, which was selected analytically and compared with initial airfoil (R-III 15.5).

Currently, there are several thousand aircraft profiles and their modifications in the world. The set of characteristics of an aviation airfoils is quite large, in most cases it is limited mainly by geometric and aerodynamic characteristics. One of the main criteria for selection of airfoil is it's aerodynamic quality which is equal to ratio of lift to drag coefficient, another was airfoil relative thickness, it must be high enough to manufacture light wing, with high enough strength and simple spar to decrease total cost. It also worth remembering about the another parameters such as moment coefficient, manufacturing simplicity etc. By this parameters three popular airfoils was selected in database Davis B24 (Fig. 2.6), R-III (Fig. 2.7) and NACA-23012 (Fig. 2.8).

R-III (15.5) airfoil wind tunnel tests were conducted by TsAGI laboratory, using the T-1 aerodynamic tube in 1932 year. They have high lift properties and good performance at high angles of attack. They were widely used in the 30s-40s, and are still in use today, this airfoils with minor modifications or without it are the base of Aeroprakt wing consoles. The advantages of the R-III profile are:

- good proven airfoil in many aircraft's designs
- linearity of lift coefficient with angle of attack;
- center of pressure is near the maximum curvature of airfoil, what is convenient in structural design and manufacturing.
- high lift coefficient

The disadvantages of the NACA-23012 profile are:

- high drag coefficient in comparison to another airfoils
- sharp flow separation on maximum angle of attack, which can decrease flight safety on aircraft without geometric or aerodynamic twist.

The contour of the NACA-23012 airfoil is formed by superimposing the smooth contour of the symmetric NACA-0012, described by a fractional-power polynomial, on the midline (along the normal to it), made up of the nose of the cubic parabola and the tail of the rectilinear part, joined without kink or break in the curvature of the contour. NACA developed this design in 1930s. It widely used in light aircraft's and helicopter blades.

The advantages of the NACA-23012 profile are:

- Its performance is super-critical, and is favored for use in airliner wings in particular, for providing high lift with low transonic drag;
- linearity of lift coefficient with angle of attack;
- suitable for use in high speed light aircraft's.

The disadvantages of the NACA-23012 profile are:

- comparatively low C_{ymax} at M 0.4;
- low values of aerodynamic quality at M 0.6;
- low values of the critical Mach number of the beginning growth of the airfoil drag in the operating range of its loading $0.2 < C_y (M) < C_{ymax}$ in cruise flight (not critical for ultralight aircraft, which maximum flight speed are quite low);
- the position of the aerodynamic focus X_f of the airfoil, variable in the values of the number M.

The Davis airfoil is used in World War II aircraft's as a base of wing design for such aircrafts as Consolidated B-24 Liberator, as well as other models. The airfoil had a lower drag coefficient than most modern designs, allowing for higher speeds and generating significant lift at relatively low angles of attack. The advantages of the Davis B24 profile are:

- low drag coefficient in comparison to other airfoils;
- can generate high lift even on low angles of attack;
- high relative thickness is convenient in structural design and manufacturing. It allows to install high capacity fuel tanks and engines in the wing;
- very smooth stall

The disadvantages of the B-24 profile are:

- not efficient in high speeds of flight, high-speed drag was strongly associated with thick wing profiles due to wave drag;

- maximum angle of attack is relatively low

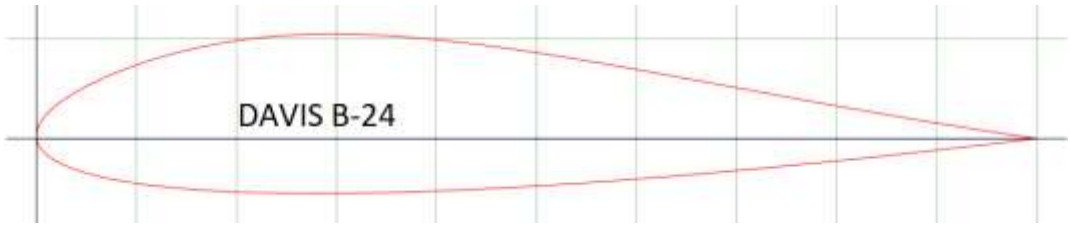

Fig. 2.6 – Davis B24 airfoil.

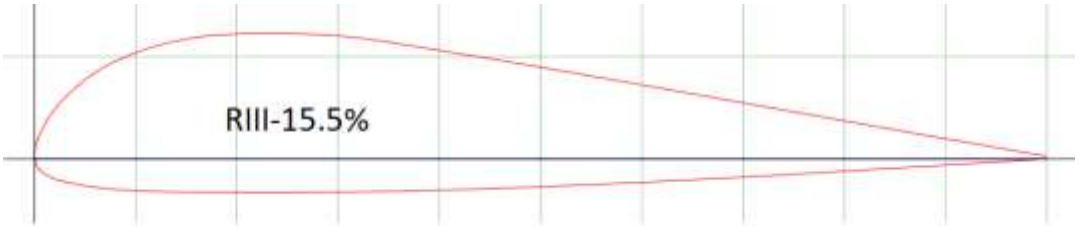

Fig. 2.7 – Davis R-III-15.5 airfoil.

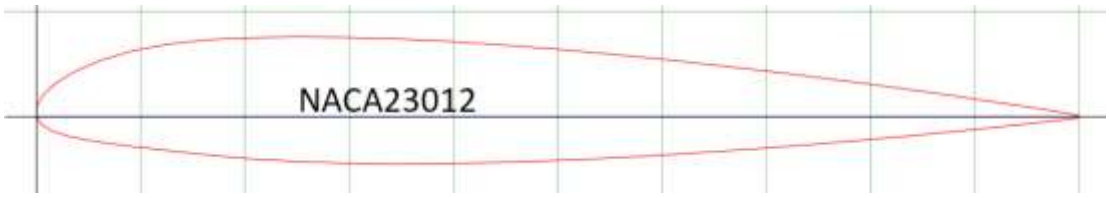

Fig. 2.8 – NACA23012 airfoil.

Polar of selected airfoils was obtained using XFLR5 software for three Reynold's numbers: 1000000, 2000000, 3000000. Mach number equal 0 (no air comprehensibility correction), the laminar to turbulent transition criterion number is set to 9, and the trip locations are set at the trailing edge. Results of calculation is shown on Fig. 2.9 (lift by drag coefficient) and Fig. 2.10 (lift coefficient by angle of attack and K quality coefficient).

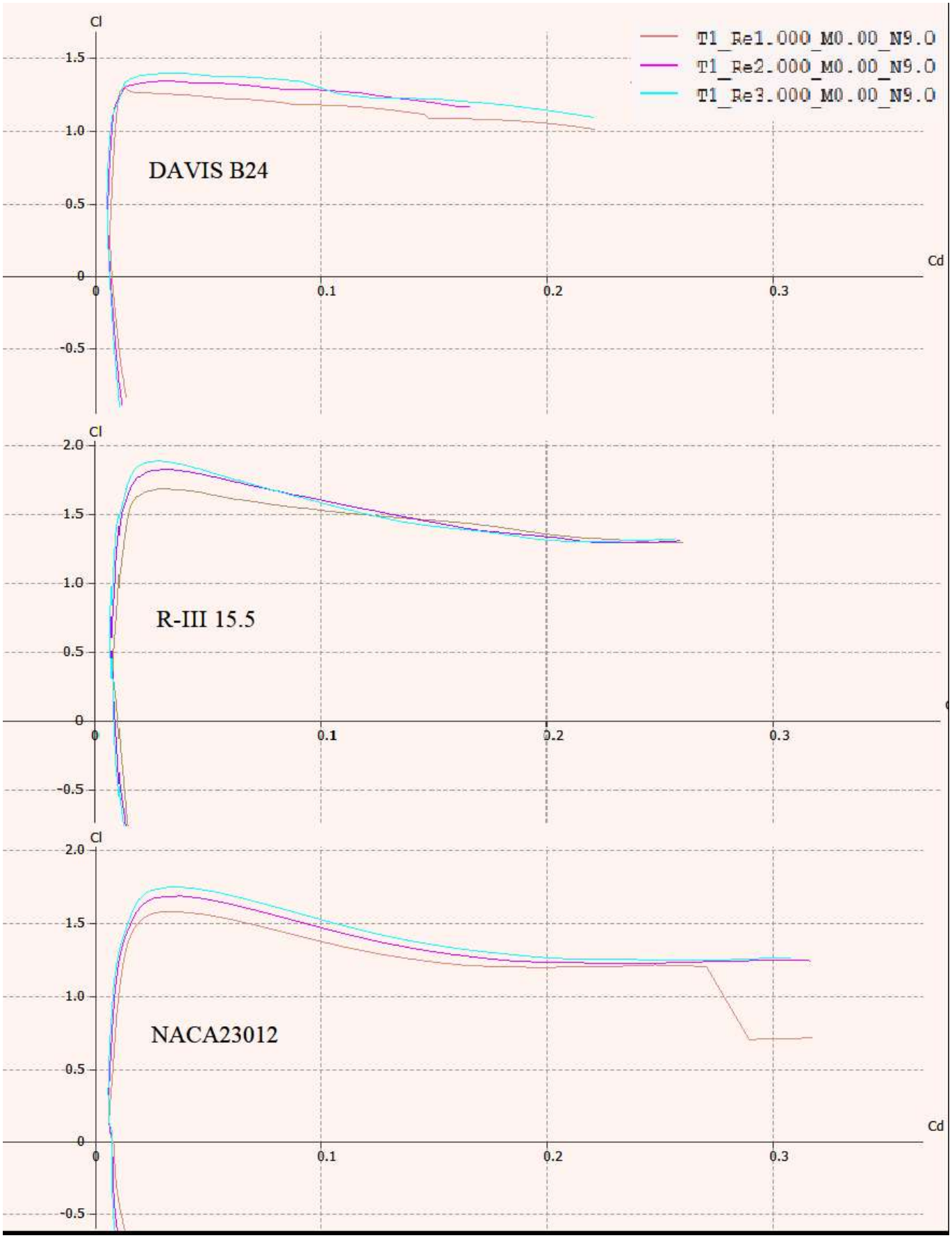

Fig. 2.9 – C_l to C_d diagram for selected airfoils

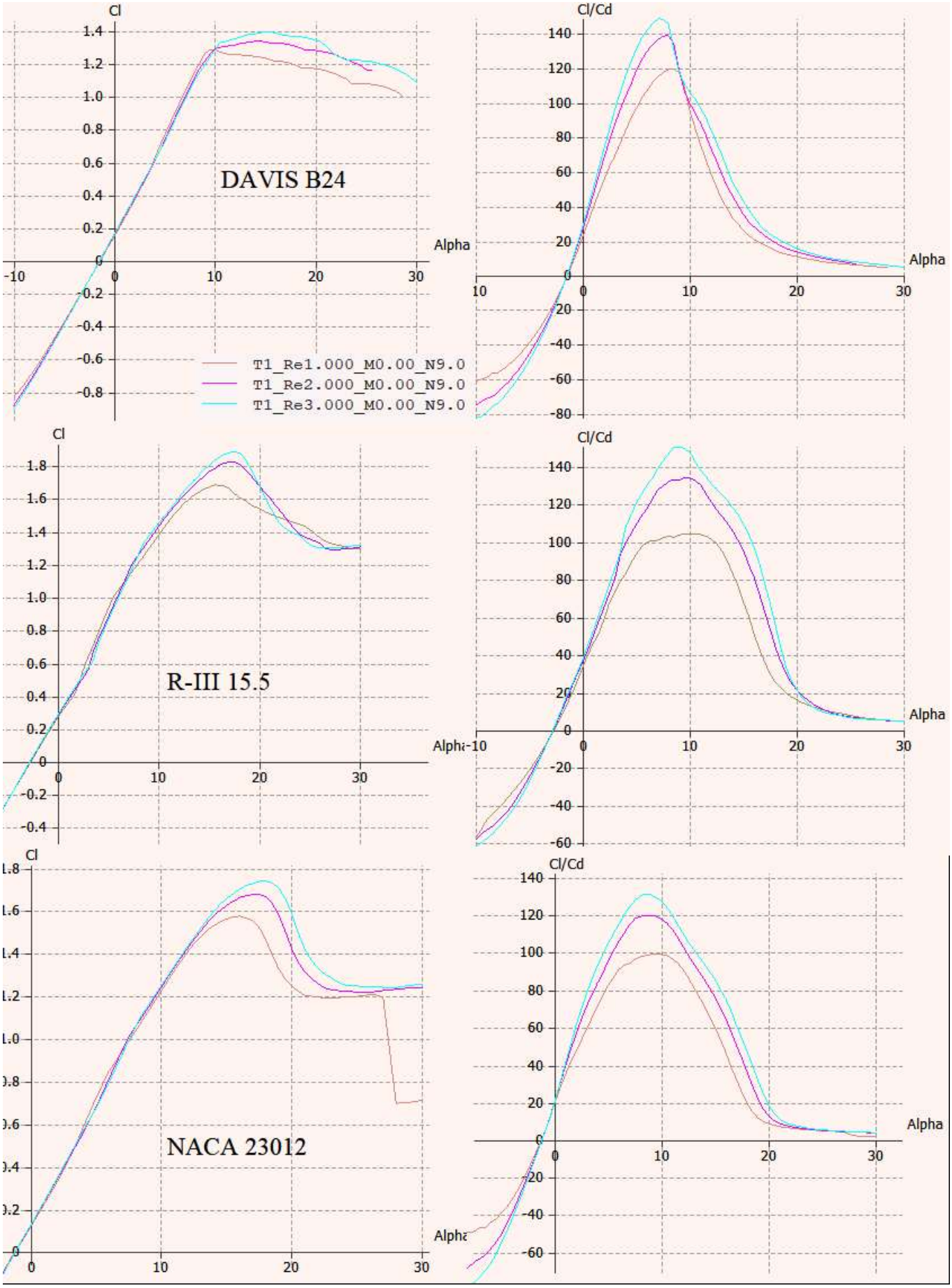

Fig. 2.10 – C_l vs Alpha and aerodynamic quality diagram for selected airfoils

Conclusion to the Part 2

Flaperons are widely used in modern light-engine aviation as a unified control surface for roll which can be used during take-off and land to significantly increase lift. A20 wing cross-section were considered in which flaperon occupy whole wing length. Results of simulation with angle of attack 15° shown increasing of C_y up to 2.24 with flap deflection angle 20° in comparison to 1.42 when $\alpha_{flap} = 0$; Which prove high effectiveness of flaps. Velocity distribution diagram shows increasing of velocity on leading edge of flaperon up to 22m/s but turbulence kinetic energy diagram confirms that supplementary energy from slot is not enough to eliminate high turbulence. Flaperons is also longitudinal control elements, which can lose it's effectiveness at high angles of attack and even lead to an accident. Those, active flow control technologies can be used to resolve this problems and increase efficiency.

Typical airfoils which can be used in light aircraft were considered. NACA23012 and R-III is widely used airfoils, which has proven in many designs. Davis B-24 was selected analytically among others in database, because it seemed promising to use for ultralight aircraft in combination with plasma actuators, which can increase it's maximum angle of attack and performances of aircraft itself. Smooth stall makes it suitable for operation at high angles of attack and in combination with flaperons. This airfoil also has high relative thickness, which decrease complexity of wing structure and and may increase strength.

Turbulence kinetic energy diagrams shows points of flow separation and it's transition from laminar to turbulent. Data from flow simulations can be used to define location of plasma actuators. Many researches with AC plasma actuators shows that for low Reynold's numbers optimal point of it's location is near the point of flow separation. In case of ns or μs DBD actuators optimal location is closer to the nose of the wing.

PART 3
ACTIVE FLOW CONTROL SYSTEM DESIGN

Research carries an appreciate value if it can be applied in practice. This section focuses on the practical application of active flow control systems, based on plasma actuator and its implementation on design. The following problems have been solved:

- investigated plasma generator integration onto existing electrical system system of aircraft, composed the basic requirements for active flow control system;
- the design of plasma generator is proposed;
- developed scheme of alternative current and ns/us pulse generator driver board;
- investigated electrical parameters of assembled driver boards, tests with restive and capacitive loads were conducted;
- composed the main requirements to aerodynamic scales for plasma actuator investigation, considered factors that influence on measurement accuracy;
- aerodynamic scales were designed and assembled for further experimental investigations.

3.1 Active flow control integration in aircraft electrical system

The aircraft's electrical system is designed to generate electricity and power onboard systems. Electrical energy is generated by the engine generator, converted by a rectifier-regulator, and supplied to consumers and the battery (24V). Consumers include engine starter, instruments, aeronautical lights, etc. Devices receive electricity through the wiring of the relevant section (depending on the current consumed), switches, and fuses. Fuses are designed to protect the electrical system and consumers from overcurrent and must be of the appropriate type and size. This system also may include measuring units, to provide information to the pilot about consumed current or battery voltage, etc.

The designed active flow control system should be easily integrated into existing systems on aircraft. A simplified circuit of an electrical system with integrated plasma generators is shown in Fig. 3.1 (circuit does not include all units and components and uses only for demonstration purposes, it is also shown some additional components which

belongs to other systems).

It is preferable to provide stabilized voltage to consumers such as instruments or sensors, because due to work of starter or generator, high voltage ripples can occur, for this purpose isolated DC-DC converter added to the system. To increase electromagnetic compatibility, galvanic isolation is the optimal solution, as it increases the accuracy of measurement, increases protection against interference. Each plasma generators also have galvanic isolation in input and output cascade.

Voltage surges may occur due to switching of electrical units, atmospheric discharges or other causes. Despite the short duration of such over-voltage, it may be sufficient for breakdown of insulation of plasma actuators dielectric layer and cause short circuit, leading to destructive consequences, due to transition from dielectric barrier discharge to arc discharge with extremely high temperature. To prevent such possibility different types of spark gaps may be used.

Generators of the most ultralight aircraft engines, such as Rotax 582 or Rotax 912, can't provide constant electrical power more than ~300W, when active flow control system may consume more than 1kW, and it's should be considered. It is worth mentioning that this system primarily active during takeoff and can be partially used to optimize flight modes, with minimum power consumption. That is why such high power on generator does not required, but battery capacity should be high enough to compensate this power lack and voltage ripples. (The battery can be thought of as a large capacitor, which is charged from the generator and compensates lack of power when it's required).

Plasma generators should be controllable, it's also should provide telemetry information to controller unit and instrumental panel about power consumption, fault messages, etc. To realize data transfer bus, CANaerospace standard was chosen. It's is a higher-level CAN-based protocol developed by Stock Flight Systems in 1998 for aeronautical applications. Now it's widely used in avionics systems on light aircraft's, UAV's and even on ISS and rockets. Physically it's a standard CAN bus, which widely used in automotive industry. Plasma generator is not a critical unit and may have only one CAN bus without reservation. The use of CAN Ground is supported by the connector pinout but strongly discouraged due to potential EMC problems in airborne applications and will not be used.

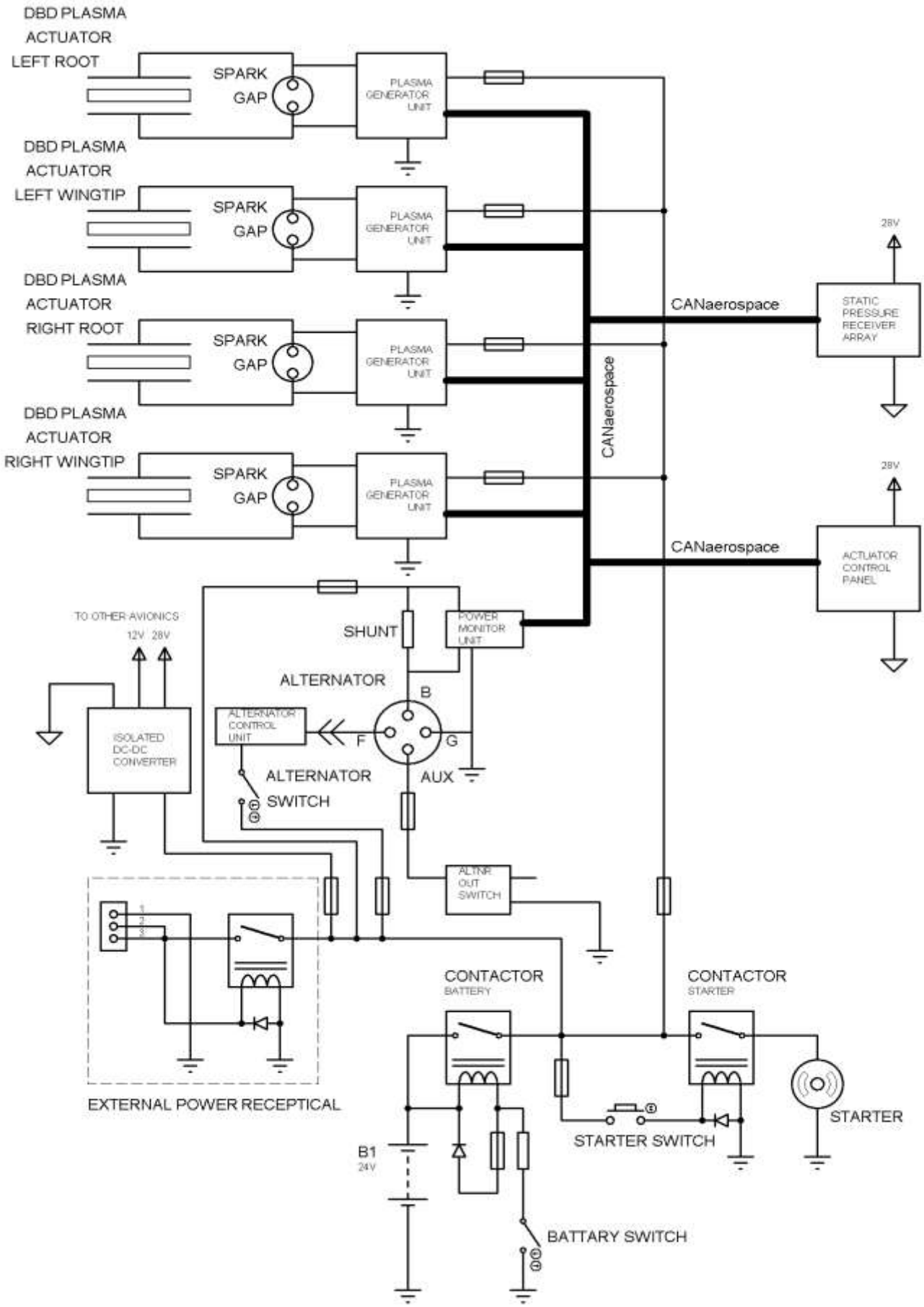

Fig. 3.1 – Power schematic

Strongly encouraged is the use of optically isolated CAN interfaces for all units in the network. For the wiring, AWG 22 aerospace standard shielded twisted pair (STP) or shielded twisted quadruple (STQ) should be used.

Plasma generators should be controllable, it's also should provide telemetry information to controller unit and instrumental panel about power consumption, fault messages, etc. To realize data transfer bus, CANaerospace standard was chosen. It's is a higher-level CAN-based protocol developed by Stock Flight Systems in 1998 for aeronautical applications. Now it's widely used in avionics systems on light aircraft's, UAV's and even on ISS and rockets. Physically it's a standard CAN bus, which widely used in automotive industry. Plasma generator is not a critical unit and may have only one CAN bus without reservation. The use of CAN Ground is supported by the connector pinout but strongly discouraged due to potential EMC problems in airborne applications and will not be used. Strongly encouraged is the use of optically isolated CAN interfaces for all units in the network. For the wiring, AWG 22 aerospace standard shielded twisted pair (STP) or shielded twisted quadruple (STQ) should be used.

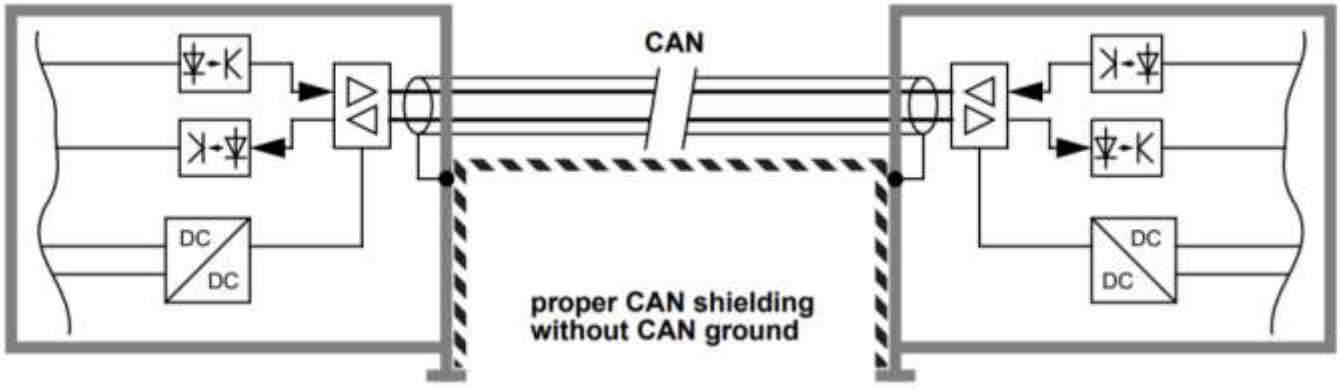

Fig. 3.2 – CAN interconnection.

As mentioned earlier, actuators should be controllable, not only switching on or off should be implemented but all other parameters (output amplitude, pulse duration, frequency, etc.) should be tuned to provide optimal operation of the system. They can be tuned manually or automatically, and the second variant is preferable. By this reason, additional element, active flow controller unit must be included in the system. It can take

flight data (aircraft relative flow speed, altitude, attitude, angle of attack, etc.) from other avionics equipment provided by CANaerospace and based on this data, make necessary tunings on plasma generators. Active stabilization of aircraft also may be implemented using this technology.

3.2 Plasma generator unit

Block diagram of ns/us plasma generator is shown on Fig. 3.3. The main task of this unit is to generate high voltage (up to 20kV) pulses with positive width from few hundred nanoseconds up to few microseconds, with short rise and fall time and with controllable frequency (near few hundred Hz).

The input of generator is connected to aircraft onboard battery. To control power consumption of each actuator, shunt in power bus should be included, it connects to current sense amplifier, or combined IC, such as Texas Instruments INA236, which has internal Analog to Digital Converter (ADC), what makes it possible to transfer current and voltage readings through digital I2C interface to Micro Controller Unit (MCU) and increase measurement accuracy.

Full bridge inverter is used to step-up input voltage up to few hundred volts, this also allows to control pulse amplitude on actuator. ST Microelectronics PWD13F60 a high-density power driver integrating gate drivers and four N-channel power MOSFETs in dual half bridge configuration is used to decrease total mass and size of board.

Rectified and stabilized DC voltage is needed to charge capacitor battery, which will subsequently discharged to the primary winding of high-voltage transformer. Resonant diode charging has found the widest application in practice. In this case, the auxiliary diode is connected to the charging circuit in series with the inductance, which prevents the return of the charge to the power supply (Fig. 3.4). With a resonant diode charging, the operating frequency of the generator can be varied within wide limits. This will change the duration of the pause t_P and at the maximum frequency $F_{max}t_P = 0$. Required capacitance C_0 to drive plasma actuator depends mainly on pulse width, transformer parameters and actuator capacitance. Knowing about C_0 value, parameters of inductance and diode can be found.

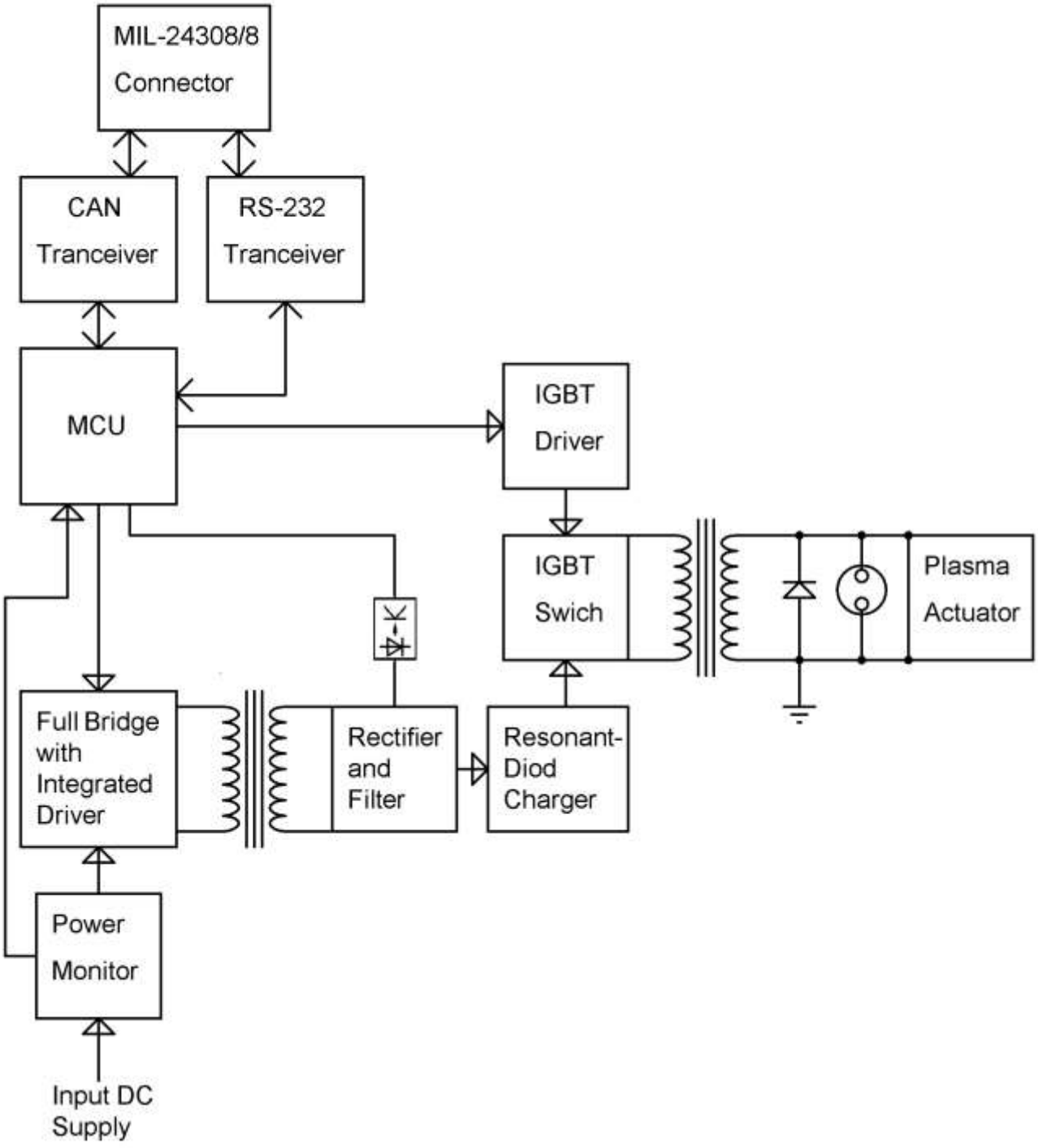

Fig. 3.3 – Generator block diagram.

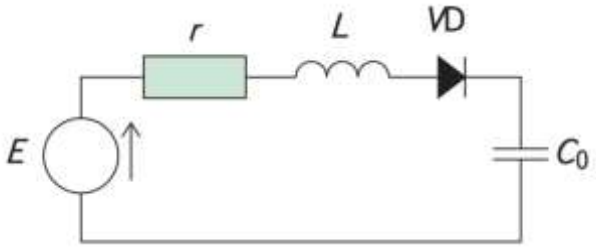

Fig. 3.4 – Resonant diode charging.

Insulated gate bipolar transistor (IGBT) semiconductor switch, which can be turned on and off periodically is used to drive high voltage transformer. Whenever the IGBT turns on, it will be turned off in a very short time. Thus, the pulses each with a pulse rising time of a hundred nanoseconds are formed by the periodical discharge of capacitor C_0 under the control of the IGBT.

A powerful and fast driver should be used to switch the IGBT with shortest rise and fall time. To fulfill this requirement and provide high reliability, was selected Texas Instruments UCC5390, single-channel isolated gate driver with UVLO. It has high sink current (10A), and very low output rise and fall time, which typically equal 12 and 10ns respectively.

Complex modern converters, such as online UPS, works under controll of DSP, MCU or ASIC. The main suppliers of DSP for power electronics are two companies, Texas Instruments and Infineon, but products of STMicroelectronics also increase influence on this market. To control all this elements, MCU with integrated High Resolution PWM (HRPWM) and ADC is a good solution to decrease unit mass and size. One of the most popular microcontrollers, which meets the specified requirements is TMS320F28335 and series of STM32F334 or STM32G4. STM32 was selected, due to it's simplicity of programming and availability. It has all required peripheral, including CAN, I2C and UART interfaces. HRPWM is familiar to PWM module, but with higher resolution of the duty cycle setting and, in addition, usually has more flexible settings.

The main tasks of MCU is to generate PWM signals for full bridge diver, duty cycle of which calculated on microcontroller core, to correspond specified voltage on rectifier, value of which reads ADC, as a feedback signal. It generates pulses to IGBT driver, control power consumption, receives and transmit messages through CAN bus.

Such design makes possible to create plasma generator not only for light aircraft, but even for small UAV.

3.3 Prototypes design

The development of effective active flow control system will inevitably face the need for experimental research. Analysis and interpretation of experimental data, their extrapolation to the conditions of the real atmosphere, as well as the actual formulation of the experiment, are mostly impossible without the use of appropriate tools for the study of flows in experimental conditions, including numerical models. The development of tools for the analysis of plasma actuators in experimental installations is an independent, valuable and urgent task. To test some components, prove efficiency and obtain some necessary experimental data, some prototypes of experimental equipment were designed and manufactured.

3.3.1 High voltage pulse generator

A high importance for the design of active boundary layer control system which based on DBD plasma actuator has power supply unit which should be used for capacitive (resonant) loads. To improve the plasma quality, high-frequency operation is essential for the promotion of plasma stability. The main task during design was simplicity of assembly, optimization of product cost and high reliability.

In general, a high-voltage pulse generator of proposed scheme consists of primary power supply, functional generator, driver board, high-voltage transformer and high voltage diode.

Scheme of driver board is shown of Fig. 3.5. Primary power source is connected to X2 connector, HSPY-400-01 programmable regulated PSU was used in tests. It charges C1 and C2 capacitors which charges array of capacitors through resonant-diode stage (L1, VD1).

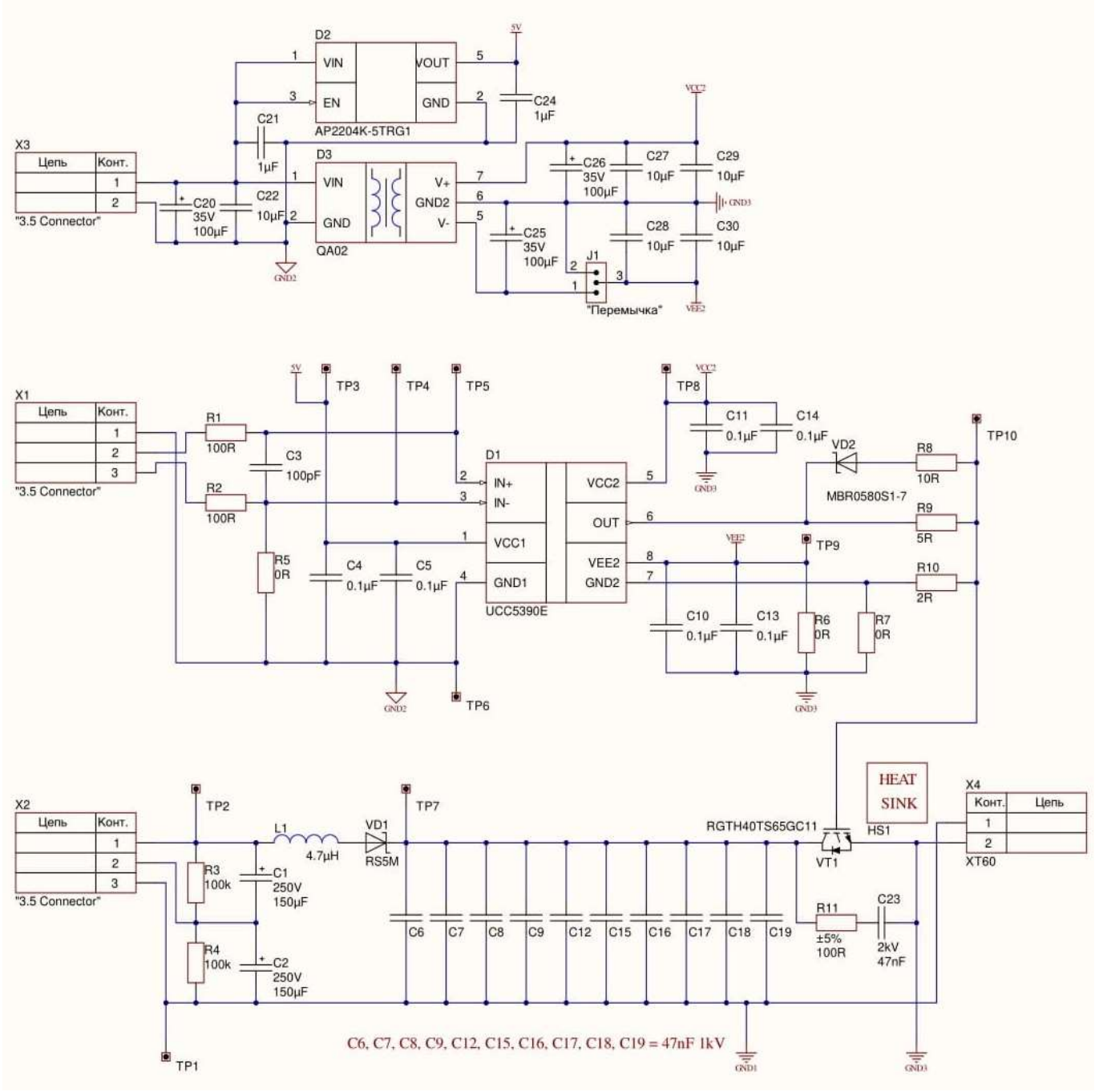

Fig. 3.5 – Pulse generator driver board schematic

STMicroelectronics STGW40NC60KD (600v, 70A, 2870pF input capacitance, 19ns current rise time and 87ns current fall time) IGBT transistor discharges capacitor array to primary winding, which connected to connector X4. It switches be IGBT driver UCC5390E, but board designed so, that any IC of UCC53xx series can be used by configuring R6, R7 and R8 resistors and J2 jumper. It operates with bipolar power supply. IGBT turns off with negative voltage on the gate with respect to the emitter. This configuration prevents power

the device from being unintentionally switched on because of current induced from the Miller effect. QA02 bipolar isolated DC-DC converter installed on board, it specially design for application with IGBT's and can provide +15 and 8.5V to driver IC. To provide stable 5V for UCC5390E low-side logic, linear regulator was used (APK2204K). For powering board, 12V power supply should be connected to X3 clamps. X1 connector is used for input signals from PWM generator. The input pins (IN+ and IN–) of the UCC53xx family are based on CMOS-compatible input-threshold logic that is completely isolated from the VCC2 supply voltage. A wide hysteresis makes for good noise immunity and stable operation.

Driver board was designed according to the standards of JLCPCB manufacturer. Four layers technology is preferable for minimization of electromagnetic interference. Additional layers are also used to increase total thickness of power rails and to provide increased isolation or gaps between tracks. Transparent PCB layout is shown on Fig. 3.6 and Fig. 3.7.

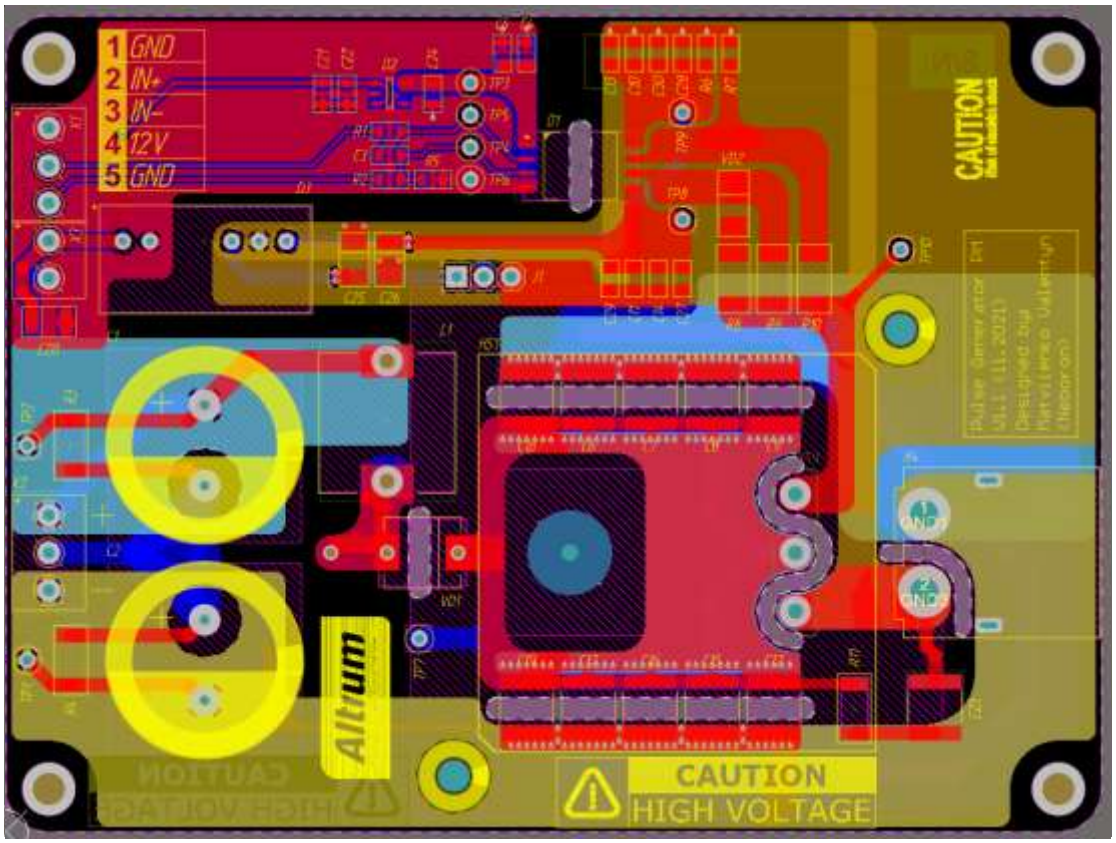

Fig. 3.6 – PCB layout (Top)

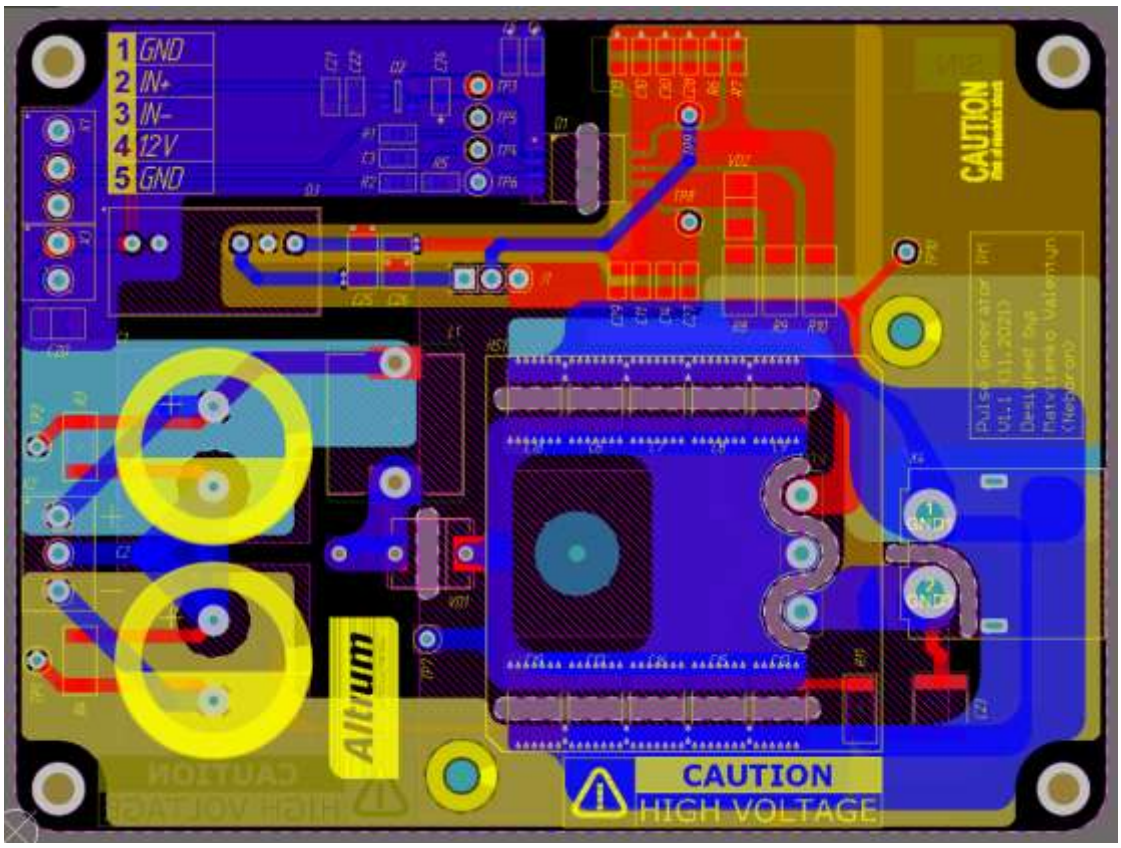

Fig. 3.7 – PCB layout (Bottom)

Final board assembly is shown on Fig. 3.8. Number and values of capacitors array is selecting according to parameters of high-voltage transformer and plasma actuator. Heat sink can be installed in case of high power dissipation from IGBT.

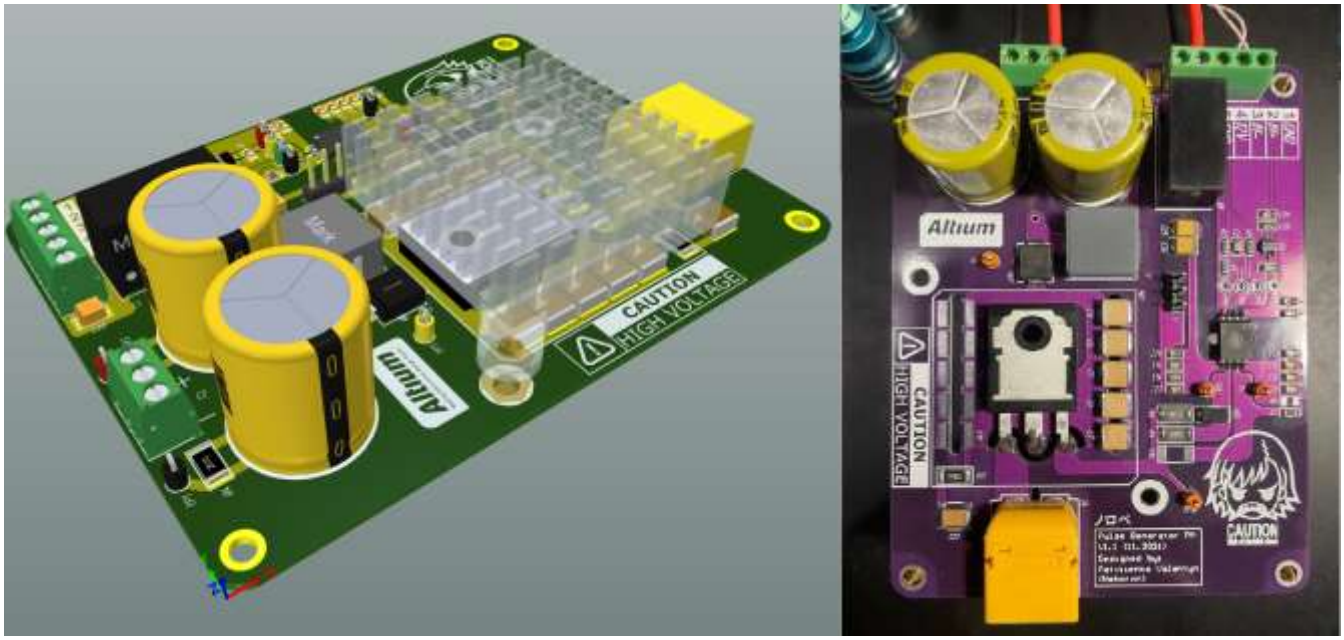

Fig. 3.8 – Board assembly

Basic tests were conducted, to evaluate main parameters of driver board. It tested with resistive (75Ω, 5W wire resistor), and inductive load (Transformer on ferite ring, 2 turns of primary coil and 20 turns of secondary). High voltage probe is Tektronix P6015 without dichlorotetrafluroethane (maximum allowable voltage was decreased to 13kV with air dielectric), probe was compensated accordance to manual. Oscilloscope is Tektronix TDS784A, low voltage and high voltage probes were calibrated before measurements. Function generator is UTG962E with approximately 15ns rise and fall time.

Oscillograms is shown on Fig. 3.9 and Fig. 3.10. Channel 1 (P6015 probe) is connected to XT60 output connector, which has resistive load. Channel 2 shows input signal on IN+ pin of driver IC from function generator (this probe has bad shielding, so some noise are present when load is connected to driver output). This results shows that generator board designed very well, and can generate enough short pulses even for use with ns DBD plasma actuators.

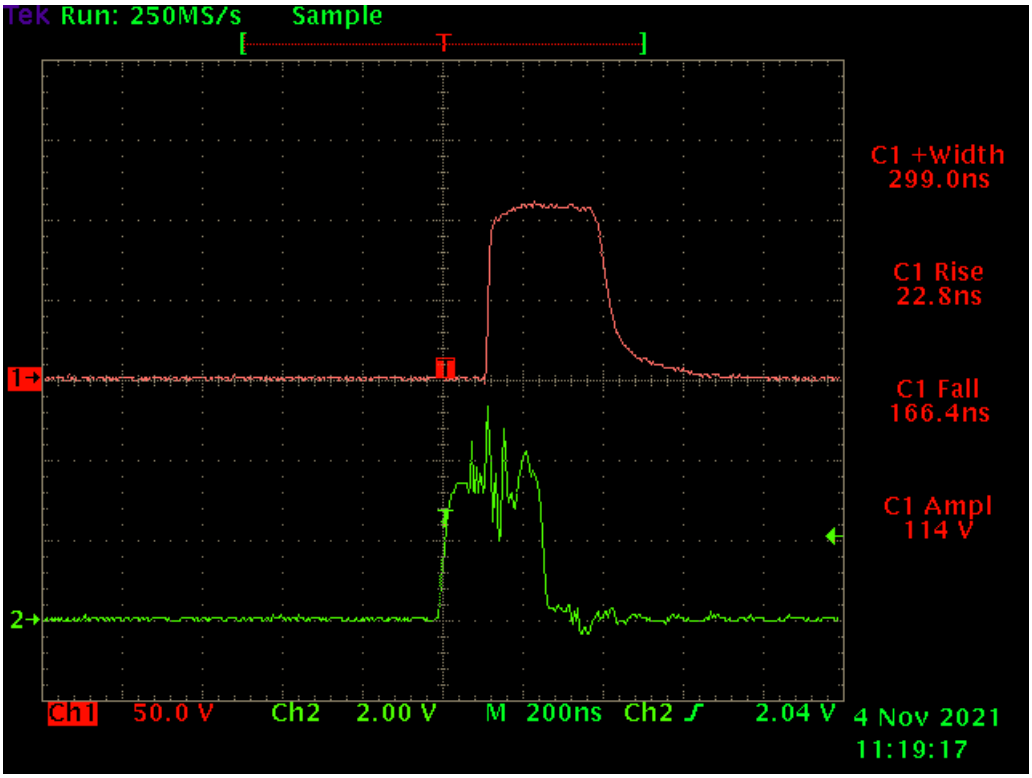

Fig. 3.9 – Oscillogram of driver board

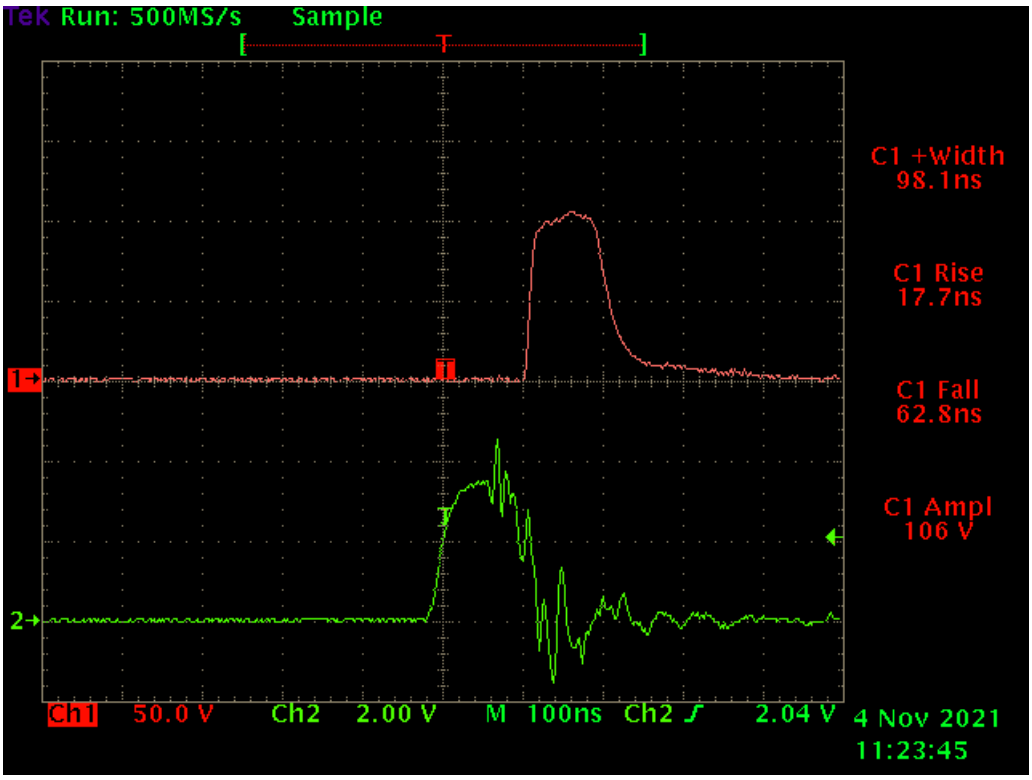

Fig. 3.10 – Oscillogram of driver board

3.3.2 High voltage AC generator

High voltage AC generator was designed and assembled to compare pulse and AC plasma actuators and for additional experiments. It consists of two boards (Fig. 3.11 and Fig. 3.12), external power supply and high voltage transformer. Components are selected such, to drive primary coil with input voltages up to 400V and frequency range from 5 to 20kHz (frequency range can be extended, such values are used for calculation of high voltage impulse transformer).

First board is a simple half bridge inverter build on MOSFET's. Supply can be by a standard laboratory power supply. UCC21520 IC used as isolated dual-channel gate driver. UCC21520 dead time setting in ns, $DT_{Setting} = 10 \times R_{DT}$(R10)(in kΩ). Converter board schematic is shown on Fig. 3.13.

Second board is PSU controller, build on STM32F334 in LQFP64 package. It mainly designed for evaluation purposes, to test all peripheral, generate PWM signals to converter board, test rise and fall time of STM32F334 series, etc. It has 5 channels of HRPWM, 10 ADC inputs, 2 independent, controllable DC-DC boost converters, CAN transceiver, 2

HPDL1414 displays, 3 buttons and 2 LED’s connected through I2C GPIO expander (for debug purpose), UART, SPI, etc.

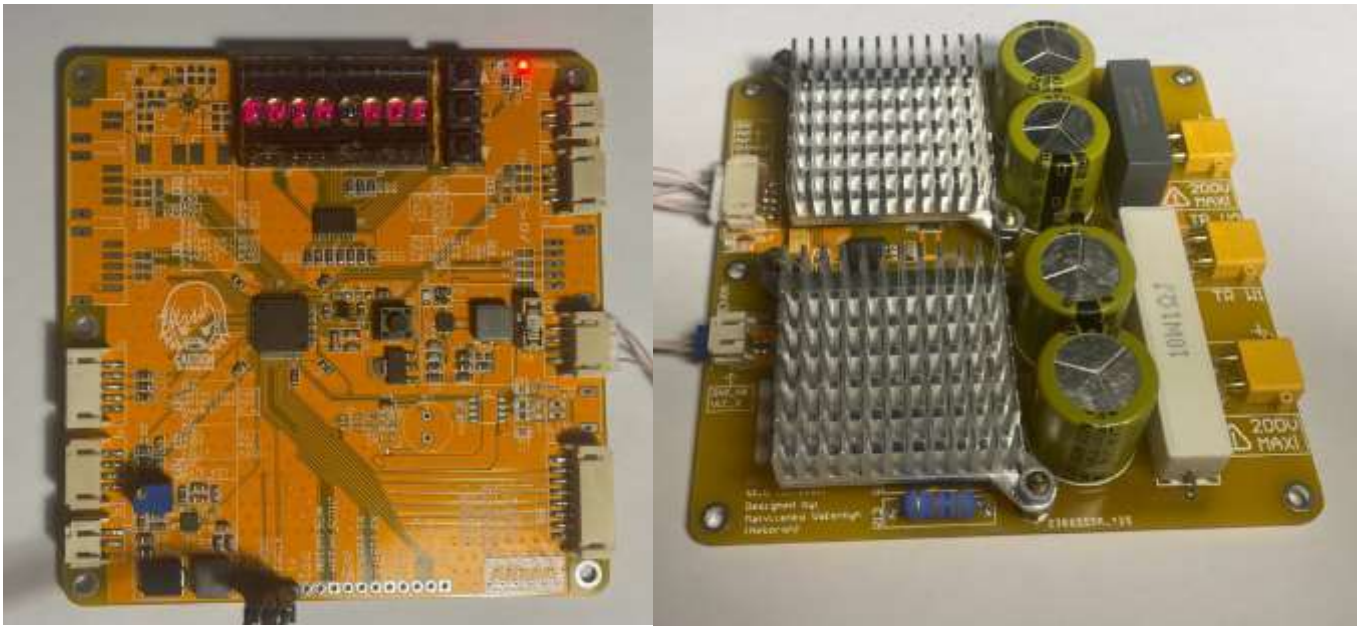

Fig. 3.11 – AC generator PCB’s.

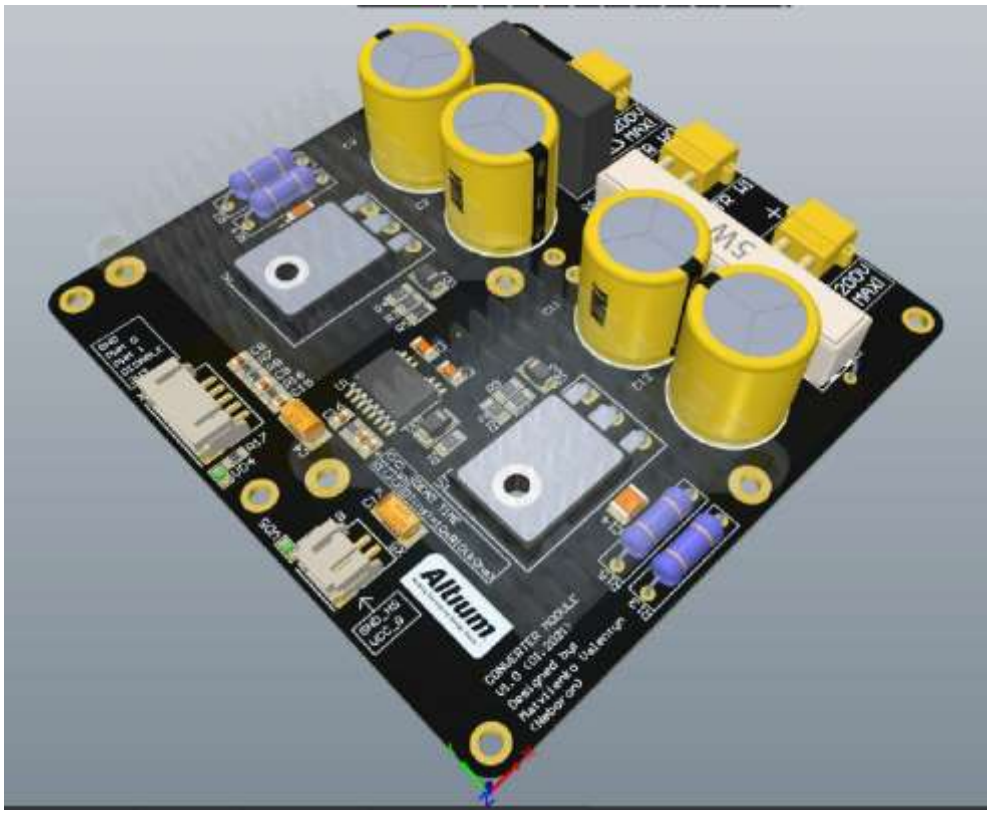

Fig. 3.12 – AC generator PCB’s.

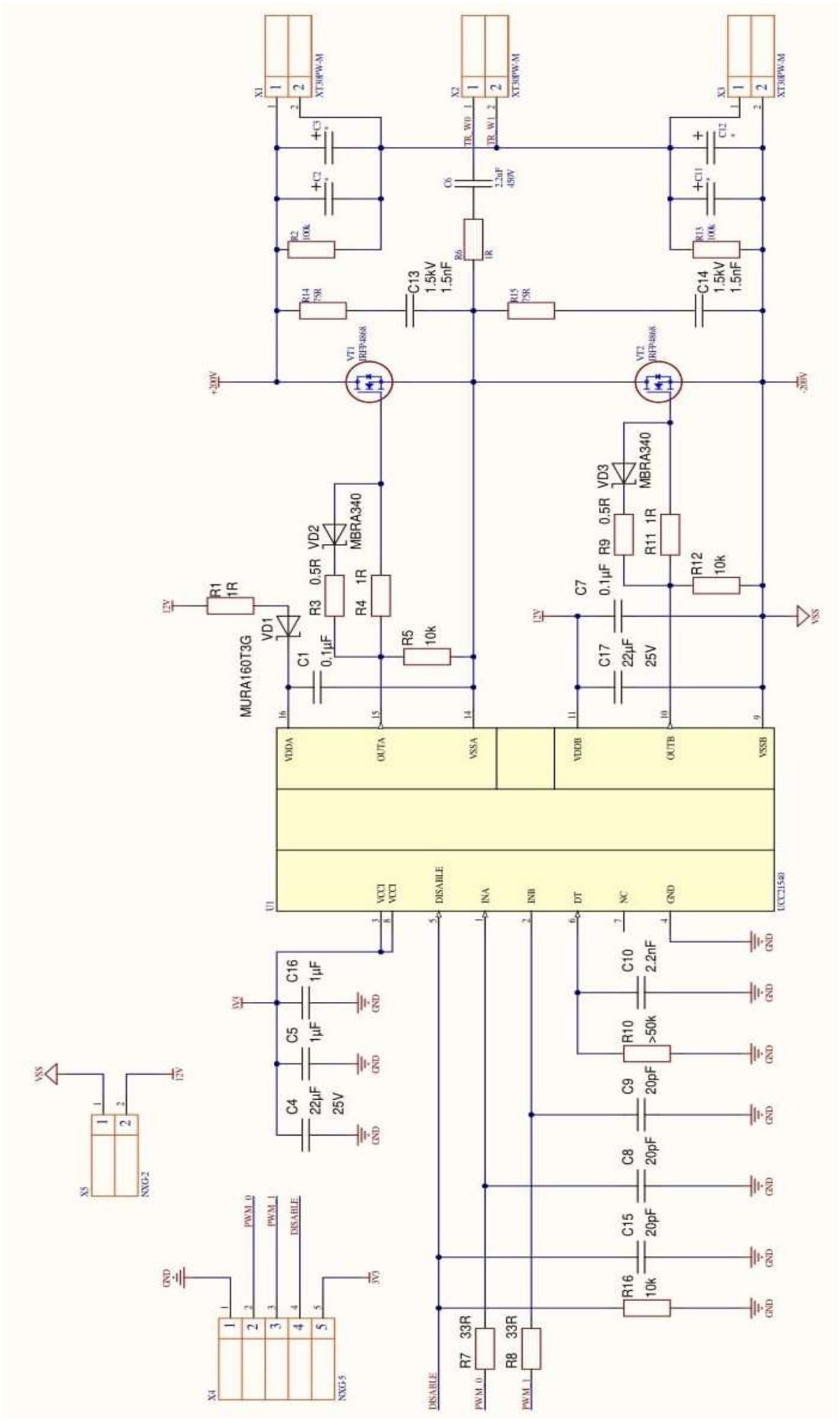

Fig. 3.13 – Converter board schematic.

3.3.3 Specialized aerodynamic scales for use with plasma actuators

Investigated in wind tunnels aerodynamic forces and moments acting on the model, can be determined indirectly by measuring pressures at many points of the model surface. A more accurate and reliable method is the direct method of measuring forces and moments using an aerodynamic scales. Unlike conventional scales used to measure force acting in a known direction, aerodynamic scales should measure not only the aerodynamic forces, the direction of the resultant of which is unknown, but also the moments of the resultant. In the most general case, the aerodynamic scales should measure the components of this resultant force in projections onto three perpendicular axes passing through any point, and three components of the total moment with respect to these axes.

The main characteristic feature of aerodynamic scales is the number of measured components. Depending on the task at hand, this number can vary from one to six. The design of the scales should provide the ability to change and measure the angle of attack, and in many cases, the model sliding angle. For most of cases, three components scales is enough for measuring lift, drag and pitch moment, it requires only mechanism to change angle of attack.

Aerodynamic scales can be subdivided into mechanical and strain gauge methods of measuring. Mechanical scales was widely used in previous century, the disadvantage of such scales is the relatively large weight of the balance elements, and due to the high inertia of the measuring systems, these scales cannot be used in wing tunnels with a very short operating time.

Strain gauge methods for measuring forces are based on the use of elastic systems, the deformations of which (proportional to mechanical stresses, and hence to forces and moments) are determined using small-sized electric strain gauges. Electrical strain gauges allow obtaining electrical signals, the values of which are the simplest functions of forces and moments. Using various electrical circuits, it is possible to transform these functions to obtain signals proportional to the components of aerodynamic forces and moments. The main advantage of such measurements is high response and simplicity of design. This type of scales was chosen for design.

The main factors which have influence on measurement accuracy is hysteresis effect, temperature variations and electrical properties of strain gauges and measurement equipment which are using in aerodynamic scales. One special factor must be taken into account when such types of scales is operated with plasma actuators, electromagnetic interference. According to the Maxwell equation, fluctuation of voltage and current can produce an electromagnetic wave. For the airborne devices, the electromagnetic wave also means EMI. The shorter the pulse rising time, the stronger the EMI will be due to the stronger fluctuation of pulse voltage.

To decrease influence of this factor, some special measures should be provided. A properly implemented grounding system significantly improves the electromagnetic environment of the room and the electromagnetic compatibility of equipment, thereby ensuring the possibility of reliable and trouble-free operation of various electronic equipment. Shielding serves as the primary means of attenuating electromagnetic interference caused by radiation. Screens are used for individual elements, assemblies, blocks and devices that can be either sources or receptors of interference. And although the load cells connected according to Wheatstone measuring bridge circuit, it's not granted that EMI can't cause high measurement errors.

Taking into account all described requirements, aerodynamic scales design was proposed (Fig. 3.14). It has two Mavin NA2 load cells to measure lift and drag force but can be easily modified for installation third load cell to measure tension and compression on rear hinge point, from which pitch moment can be obtained. Maximum allowable load for each axis is equal 60kg force. All metal mechanical parts are interconnected and can be easily grounded. Additional shielding covers is used to protect load cells from EMI, all cables are also has double shielding which minimize electromagnetic influence on measuring equipment.

High voltage cables is soldered to special PCB's with 1.6mm thickness of FR4 material, which used for wing mounting and to supply energy to plasma actuator. Special model connector unit was design for easily interchangeability of blown models and connecting it to high voltage bus. Connector unit has enough powerful magnets in rear part to securely restrain blown model during wind tunnel tests.

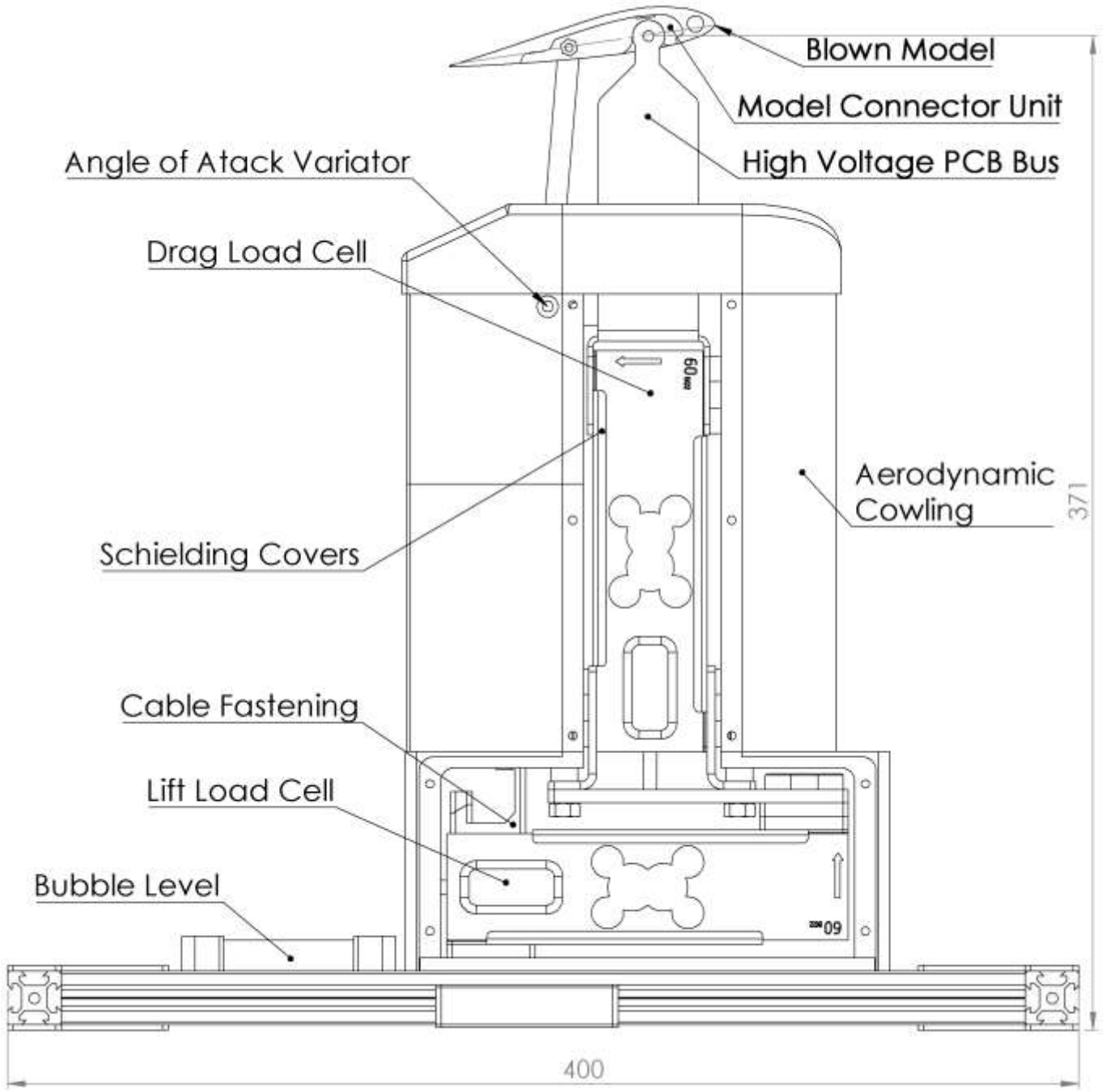

Fig. 3.14 – Aerodynamic scales design (side view).

Model connector unit designed so, to provide angle of attack changing from -10° to +35° which covers most of possible tasks. It can be changed manually by clamping screw of rear hinge linear guide. Aerodynamic cowling is designed to minimize parasitic drag from structural components of scales, only wing mounting supports and rear plate locates in flow, which drag can be easily find and taken into account during calculations.

Assembled aerodynamic scales is shown on Fig. 3.15 and Fig. 3.16.

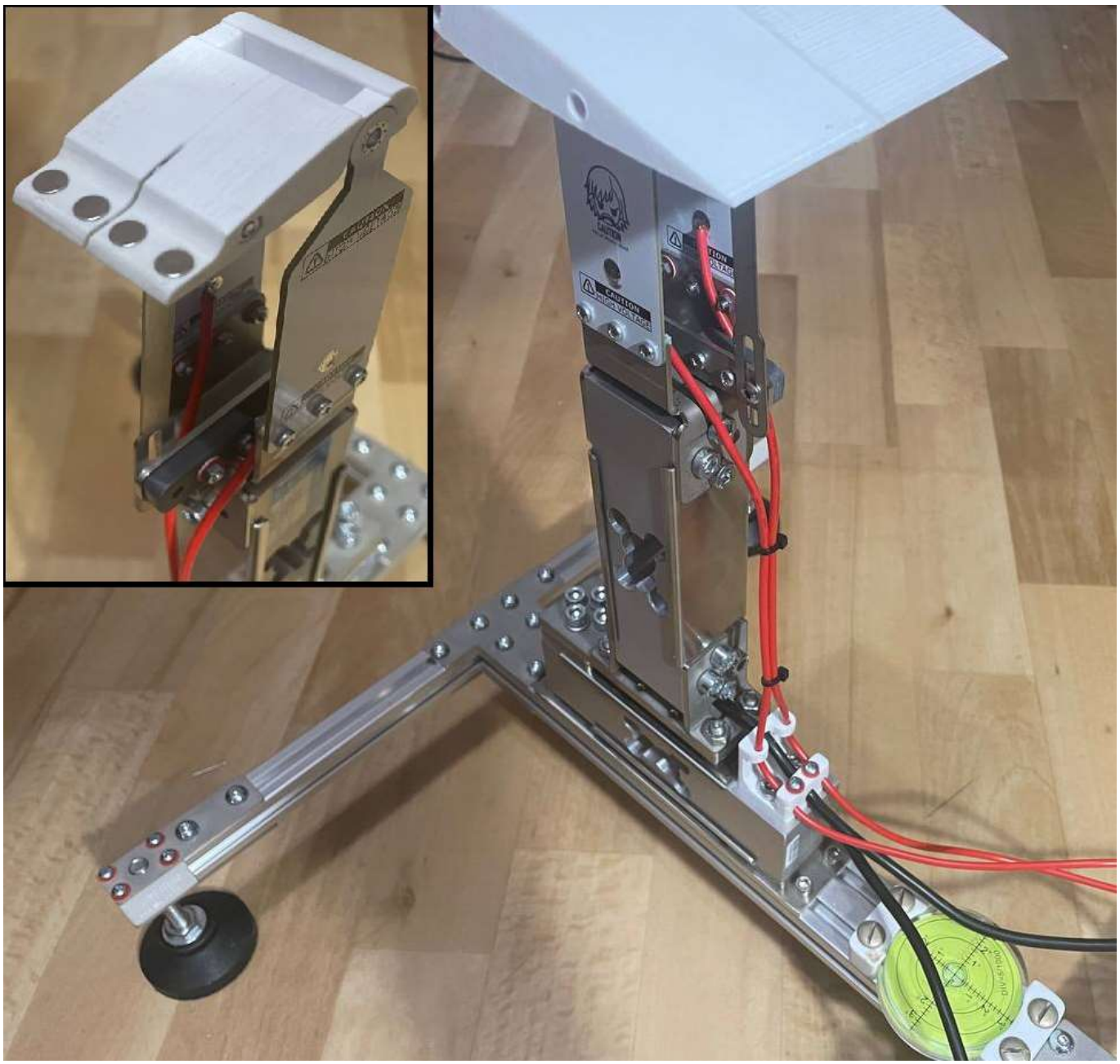

Fig. 3.15 – Aerodynamic scales assembly (without cowling).

Scales was specially designed for parameters of UTAD-2 aerodynamic wing tunnel, which located in National Aviation University. UTAD-2 is a closed atmospheric wind tunnel with an open working part of the elliptical section 700×450 mm. Distance from floor to ellipsoid center is equal 1200 mm and laboratory table height is equal 740 mm. It used to conduct training laboratory classes, as well as research and metrological certification of anemorumbometers. UTAD-2 is also used for methodological tasks: testing of experimental installations, testing tasks and data processing, which are further implemented on the wind tunnel TAD-2.

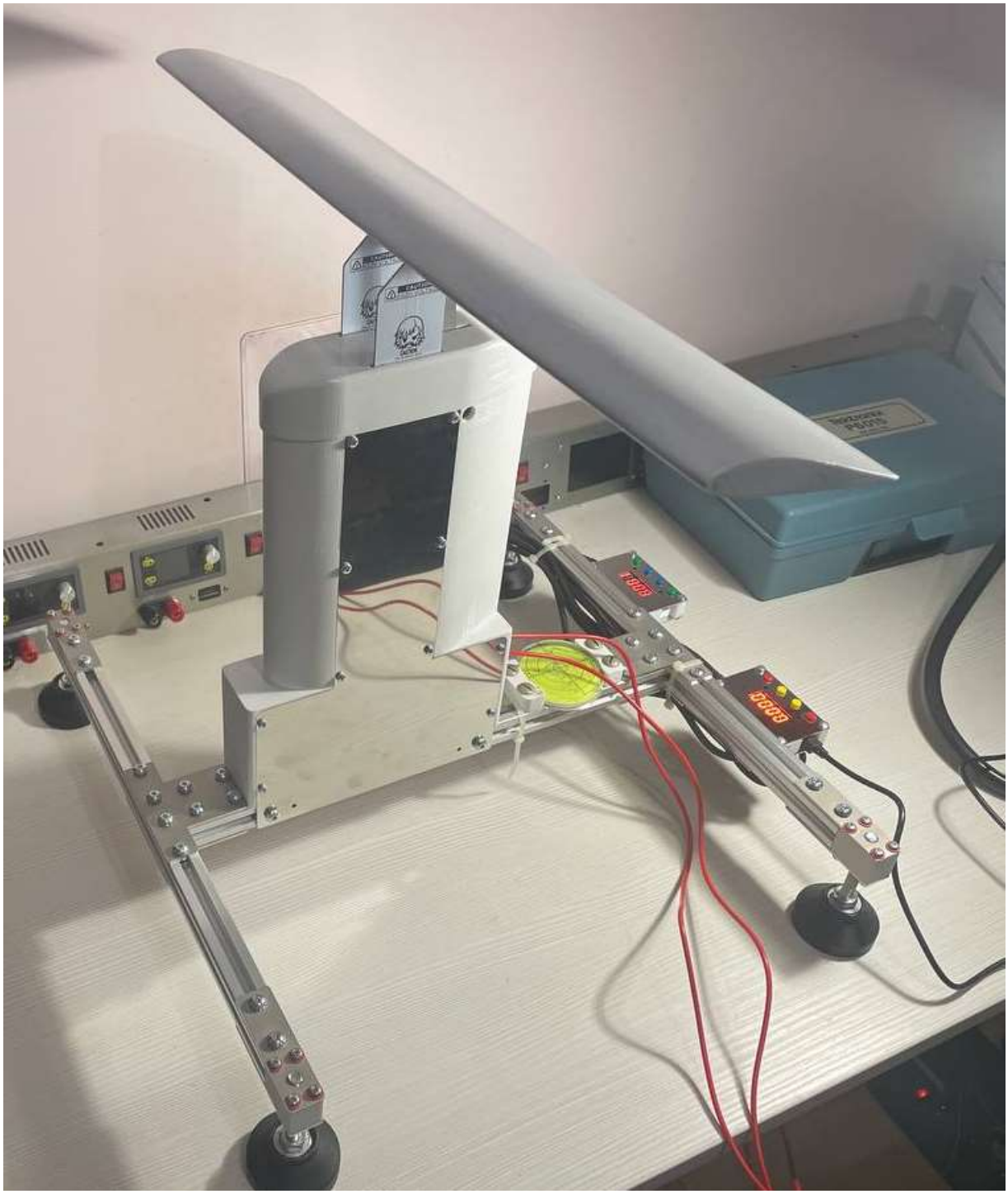

Fig. 3.16 – Aerodynamic scales assembly (with cowling and installed model).

HX710 specialized analog to digital converter were used to measure voltage difference on Wheatstone bridge. Measurement equipment were calibrated before use with weights of the fourth accuracy class. Static load tests showed that measurement error is not more than 2g in range of loads from 0 to 2 kg force.

Conclusion to the Part 3

Flow separation is an important problem in aviation field. Once it has been occurred, great lift will be lost and drag will increase. Therefore, the flow separation control is important for the better performance of aircraft. By this reason, the main task of this part was design of active flow control system, and its integration.

Plasma actuator system should be easily integrated into the existing aircraft design with minor modifications, an integration example was shown on Piper Archer 3 electrical system schematic. Plasma generator design was proposed. For its operation in the flight, the μs-DBD can be used due to both its flow control ability being similar to the ns-DBD and the reduced EMI.

To verify the practical application capability of plasma actuator flow control system and simulate the function of typical slats and ailerons, tests should be conducted. For such verification's special equipment were designed and assembled. Laboratory tests of pulse plasma generator were conducted, which shows possibility to generate high voltage pulses of established frequency and duration for most of μs-DBD configurations. 18 ns rise and 63 ns fall time makes it suitable even to generate pulses for ns-DBD actuators with minor modifications.

Designed and assembled aerodynamic scales open up opportunities to evaluate plasma actuators performances with with high enough accuracy and minimum influence of electromagnetic interference on measurement results. Designed connector unit provide endurance connection of plasma actuator to power rails, it also may significantly decrease time between tests, due to possibility of model quick replacement and angle of attack adjustment simplicity.

PART 4
LABOR PROTECTION

4.1 Introduction

To obtain results about actual efficiency and another performances of pulse plasma generator and dielectric barrier discharge plasma actuators, prototype, special equipment should be manufactured and some experimental investigations may be conducted. Such equipment use extremely high voltage sources (>10 kV peak to peak for actuators, etc.) which may cause serious injury or even be fatal. Other dangerous factors is the increased level of electromagnetic radiation and generation of ozone in high concentration. The subject of this work is an engineer who works with such equipment. In this chapter will be considered working conditions in aerodynamic laboratory and some precautions for it's workers.

4.2 Analysis of working conditions

The health and performance of a person in the labor process is influenced by a combination of factors of the working environment and the labor process. Depending on the quantitative characteristics and duration of action, certain harmful production factors of the working environment can become hazardous. From a variety of hazards and stress factors, consider their characteristics and established norms.

During the work with plasma actuators next possible physical hazardous and harmful factors according to GOST 12.0.003-2015 should be considered:

- increased noise level in the workplace;
- increased air ionization;
- an increased voltage value in an electrical circuit, the closure of which can occur through the human body;
- increased level of static electricity;
- increased level of electromagnetic radiation;

4.3 Organizational and constructive-technological measures to reduce the impact of harmful production factors

Methods of protection against electric shock. Protection of the person against influence of contact potential and currents is provided by a design of electric installations, technical ways and means of protection, organizational and technical actions are made accordance to DSTU 7237.2011. The following methods and means must be used to protect against accidental contact with live parts:

- protective shells;
- protective fences (temporary or permanent);
- safe location of live parts;
- insulation of live parts (working, additional, reinforced, double);
- workplace insulation;
- low voltage;
- protective shutdown;

Insulation of conductive parts of electrical installations, and in special cases double or reinforced, prevents the occurrence of current on metal non-conductive parts of electrical equipment, leakage to earth, and protects a person from exposure to electric current when accidentally touching live parts. On designed equipment were applied some methods to protect human from electric shock. For example, all wiring which connects actuator and plasma generator is double, reinforced wires which can provide isolation up to 30kV, step-up high voltage impulse transformer filled with epoxy resin, which also provide high isolation. But some parts, can’t be isolated, or covered on protection fences, for technical reasons. Those parts are marked with caution signs (Fig. 4.1a and Fig. 4.1b). All body parts of equipment is interconnected and should be grounded to reduce electromagnetic influence and to provide protection against electric shock when touching metal non-current-carrying parts that may be energized as a result of insulation damage.

Fig. 4.1 – a) Caution signs on wing bracing which has high voltage rails; b) Caution sign on driver board (voltage on some components up to 500VDC)

Methods of protection against electromagnetic field. According to DSTU B A.3.2-14: 2011 The EMF voltage in the frequency range 60 kHz-300 MHz at the workplaces of staff during the working day should not exceed the established maximum permissible levels (GDR):

by electrical component, V / m:

- 500 for frequencies from 60 kHz to 3 MHz
- 300 for frequencies above 3 to 30 MHz
- 80 for frequencies over 30 to 50 MHz

by magnetic component, A / m:

- 50 for frequencies from 60 kHz up to 3 MHz

Increased levels may be allowed, but not more than twice in cases where the time of EMF impact on staff does not exceed 50% of the working day.

Reducing the intensity of the EMF in the microwave working area can be done by shielding the radiation sources with solid metal and mesh screens. The intensity of the radiation can also be reduced with the help of absorbent coatings. The electromagnetic field in the metal screen induces eddy currents that create an EMF opposite the screen.

Shielding of the workplace is provided in those cases when the reduction of radiation intensity directly near the source or its shielding causes technical complications. Workplace shielding is performed in the form of an open screen or a special cabin, from where you control the work or setup of the installation.

Absorbing screens (coatings) are used in cases where the reflected electromagnetic energy from the inner surfaces of solid metal screens can significantly disrupt the operation of the microwave generator. Therefore, absorbent coatings should fully absorb energy if possible. This is achieved by appropriate selection of the dielectric and magnetic permeability of the absorbent material.

Methods of protection against increased air ionization. Ions in the air can be formed due to natural, technological and artificial ionization. In plasma actuators air ionized due to high potential between electrodes (artificial ionization). Formed ions propagate mainly in the immediate vicinity of the technological installation.

The characteristics of ions are movability and charge. The movability of ions is expressed by the coefficient of proportionality "K" (cm/sec - cm/v) between the velocity of ions and the electric field strength acting on the ion. The movability of ions depends on their mass: the greater the mass, the lower the speed of movement of the ion in the electric field. According to movability, the whole spectrum of ions is conventionally divided into five ranges:

- lungs $K \geq 1,0$;
- average $1.0 > K > 0.01$;
- heavy $0,01 > K > 0,001$;
- Langevin ions $0.001 > K > 0.0002$;
- super heavy ions $0.0002 > K$;

Each ion has a positive or negative electric charge (polarity).

Depending on the ratio of ionization and deionization processes, a certain degree of air ionization is established. The degree of ionization of the air is determined by the number of ions of each polarity in one cubic centimeter of air. The number of ions and their polarity are determined by ion counters. The polarity index is calculated from the measurement

results. The polarity index P is the ratio of the difference between the number of ions of positive (+) and negative (-) polarity to their sum:

$$P = \frac{n^+ - n^-}{n^+ + n^-} \quad (5.2)$$

These regulations regulate the amount of light ions only. The following norms are set as regulated indicators of air ionization:

- the minimum required level;
- optimal level;
- the maximum allowable level;
- polarity indicator.

The minimum required and maximum permissible levels determine the range of ion concentrations in the inhaled air of the named premises, deviation from which will pose a threat to human health.

Normative values of air ionization in industrial and public areas shown in Table 4.1.

Table 4.1 – Normative values of air ionization

Levels	Number of ions in 1cm^3 of air		P
	n^+	n^-	
Minimum required	400	600	-0,2
Optimal	1500-3000	3000-5000	from -0,5 up to 0
Maximum allowed	50000	50000	from -0,05 up to 0,05

To decrease air ionization or normalize the ionic regime of the air environment, it is necessary to use the following methods:

- supply and exhaust ventilation;
- increase distance between workplace and the zone with an unfavorable level of ionization;

4.4 Calculation of artificial lighting in the workplace

The task of the calculation is to determine the type and number of lamps to create a given illumination in the workplace or to determine the illumination that we expect on the work surface with a known number and power of lamps.

Designing lighting facilities, next factors should be considered:

1. Choose a lighting system. It is known that the combined lighting system is more economical, but in hygienic terms, the general lighting system is more modern, as it distributes light energy more evenly.

2. Determine the normalized lighting in the workplace. To do this, you need to know the nature of the work performed. With the minimum size of the object of distinction, evaluate the contrast of the object of distinction with the background and the background in the workplace and in Appendix 1 in accordance with the selected lighting system and light source to find the normalized illumination.

Three methods are mainly used to calculate artificial lighting: the luminous flux utilization factor method, the specific power method, and the point method.

For calculation of the general uniform illumination at a horizontal working surface the method of a factor of use of a light stream acts as the basic. Luminous flux of lamps is calculated by the formula:

$$F = \frac{E*S*K*Z}{N*n*\eta} lum, \quad (5.2)$$

where E is the normalized minimum illuminance, lux;

S is area of the illuminated room, m^2;

Z is illuminance non-uniformity coefficient is equal to the ratio, the value of which is usually within 1.1…, 1.5;

K is stock ratio, the value of which is in the range of 1.5… 2.0;

N is number of lamps;

n is the number of lamps in each lamp;

η is the luminous flux utilization factor of the lamps, which depends on the room index, the distribution curve of the luminaire group and the luminous flux reflection coefficient from the ceiling, walls and work surface.

The index of the room is calculated by the formula:

$$i = \frac{A*B}{h_p(A+B)}, \quad (5.3)$$

where h_p - the distance from the lamp to the work surface, m;

A, B - respectively the length and width of the room, m.

Having determined the luminous flux *F* select the nearest standard lamp according to GOST 6825-91 (IEC 81-84) "Fluorescent tubular lamps for general lighting".

Input data:

A = 8m (laboratory length);

B = 6m (laboratory width);

h = 3.5m (laboratory ceiling height);

K = 1.3 (reserve coefficient for fluorescent lamps);

Z = 1.3 (illuminance non-uniformity coefficient);

p_n = 70 (ceiling reflection coefficient);

p_c = 50 (walls reflection coefficient);

p_p = 20 (working surface reflection coefficient);

h_c = 0.8 (mean working surface height).

Based on the input data, area of the room and the height of the lamp above the work surface can be found:

$$S = A * B = 48m^2; \quad (5.4)$$

$$h_{\text{р}} = h - h_c = 2.7\text{м}. \quad (5.5)$$

Distance between the rows of lamps and the number of lamps can be calculated as:

$$L = 1.5 * h_p = 4.05\text{м}; \quad (5.6)$$

$$N = \frac{S}{L^2} \approx 3. \quad (5.7)$$

Number of lamps in electrolier is equal 2. Index of the room:

$$i = \frac{S}{h_p(A+B)} = 1.27. \quad (5.8)$$

According to the table of luminous flux utilization factors for illuminator with fluorescent lamps:

η =0.32 (luminous flux utilization factor)

Normal illumination according to DBN B.2.5-28-2006 "Natural and artificial lighting":

$$E_n = 200 \text{ lx}$$

Luminous flux of lamps is equal:

$$F = \frac{E_n * S * K * Z}{N * n * \eta} = 8450 lm. \quad (5.9)$$

Lamp which is suitable to a certain light stream of lamps can be choosen, considering deviation of a light stream -10…+20%. Fluorescent lamp 105W 4500K E27/E40 with luminous flux FP = 8350 fits the calculated result.

Determine the actual illuminance of the room:

$$E = \frac{F_p * N * n * \eta}{S * K * Z} = 197 lx. \quad (5.10)$$

4.5 Fire safety

Measures considered in accordance with the requirements of DBN A.3.2-2-2009 on fire prevention and fire protection, as well as measures in accordance with the requirements of DSTU 7113: 2009 on explosive surroundings. Fire and explosion safety is the state of an object in which the occurrence of fire and explosion is excluded, and in case of occurrence, the action of dangerous factors of fire and explosion on people is prevented.

The laboratory in which the plasma generator is used has a fire safety category D. Despite the low level of danger in the room, electric current can cause a fire due to damage to insulation, poor electrical wiring or short circuit. To avoid dangerous situations, electrical equipment is equipped with an automatic overload protection and short circuit protection. The room is also equipped with a hand powder fire extinguisher. Powder fire extinguishers OP-1, OP-25, OP-10 are used to extinguish small fires of flammable liquids, gases, electrical installations with voltage up to 1000 V, metals and their alloys.

The room is also equipped with means of notification in case of fire. To do this, a fire alarm sensor is installed on the ceiling.

Conclusion to the Part 4

In this part of the thesis, the main regulatory documents were considered, the data of

which must be taken into account in the design and arrangement of the workplace.

A result of the analysis, harmful and dangerous factors were identified that affect the engineer during work: possibility of electric shock, insufficient light, high levels of electromagnetic radiation. Provided recommendations for improving the working conditions of the engineer for the operation of equipment, as well as measures to normalize the lighting of the work area.

PART 5
ENVIRONMENTAL PROTECTION

5.1 Ultralight aircraft manufacturers in Ukraine

At the end of the sixties in the USA, Western Europe, and in the seventies in the USSR, a new direction in the development of aviation technology was formed, called ultralight aircraft. In 1981, the International Aeronautical Federation (FAI) determined that this type of aircraft includes single and double airplanes with an empty mass not exceeding 150 kg. Other restrictions also have been identified. Now this mass was increased and depends on the country where this aircraft will be operate.

The interest to ultralight aircraft increased due to their wide capabilities for solving educational, sports and economic tasks, also due to emergence of modern materials and technologies, powerful and economical engines.

Ukrainian private designers and companies successfully design, manufacture and sell approximately two hundred ultralight aircraft a year that fly around the world. Many of this designers and engineers come from giant companies such as Antonov or Motor Sich where they gained a lot of experience in heavy aircraft design.

The Ukrainian company Aeroprakt has been producing ultralight two-seats aircraft weighing up to 600 kg for 25 years. Today, more than a thousand of them fly around the world.

In the early 1990s, designers Yuri Yakovlev and Oleg Litovchenko, created the production of aircraft actually in the garage. The first manufactured aircraft took off in 1993. In the 90s, the company built up a base and released several aircraft a year.

Now Aeroprakt has an industrial site in Kiev for 2000 square meters, Nalivaikovka airfield and more than 80 employees.

Aeroprakt constantly increases production volume and now the annual turnover approached more than 5 million euros. Aeroprakt's production volume is 5% annual volume of the world market of ultralight aircraft’s. In total, during its history, the Ukrainian manufacturer has produced more than 1,200 aircraft.

The company specializes in the production of ultra-light two-seat high-wing aircraft. The line includes two basic models: the classic "ultralights" A-22 (Fig. 4,1) and A-32 (Fig. 4,2), which are divided into two sub-models with different take-off weights. Aeroprakt also produce another aircrafts which even include triple-seat seaplanes but in much less quantity. The planes are equipped with Rotax engines, they are fueled with regular gasoline and can fly a distance of 1,100 km at a speed of up to 180 km / h. They consumes not more than 25 l/hour of 95 gasoline in maximum RPM and 15-20 l/h during cruise flight.

Fig. 4.1 – Aeroprakt A22

Fig. 4.2 – Aeroprakt A32

A representative office of the German company Flight Design operates in Kherson. The Ukrainian company provides assembly, and the aircraft's are sold all over the world. Until recently, the company was the leader in the production of light two-seat sports aircraft worldwide, producing about 200 aircraft per year. Now, produces 50-60 aircraft a year.

Flight Design CT includes seweral models, one of the most popular CTSW shown in Fig. 4.3.

Fig. 4.3 – Flight design CTSW

Another company, Aeros specializes in paragliders, hang gliders, motor hang gliders and light aircraft (as kits). The manufacturer sold about 50 kits last year and the same amount of other equipment.

A 5-seater monoplane LA-50 ANG (Fig. 4.4) was firstly presented on exhibition in 2016 by Patriot UA company which has been developed in Brovary since 2014. The enterprise has a design and engineering department and an airfield. The company has presented a new model, called ANG 01, which is based on LA-50. Which also equiped with Rotax 915 iS3A 141 HP engine. At the same time, the ANG 01 is significantly more advanced than its predecessor. Thus, thanks to the use of new carbon fiber materials, its weight has been reduced and its strength characteristics have been improved. Empty weight of aircraft is 380-400 kg (maximum configuration), and a maximum take-off weight of 950 kg. Thus, the payload is 550-570 kg, that is, 137% -150% of its own weight. This aircraft not classifies as ultralight but due to its weight, which is close to ultralight category, it presented here. Currently is preparing for serial production.

Fig. 4.4 – Patriot LA-50 ANG

Softex Aero company based in Brovary which produce helicopters, added light planes to their line: VP-12 and V-24-I. VP-12 is double-seat aircraft equipped with Rotax 912 engine. By the request of customer, it can constructed is several categories according to the rules CS-22 as moto-glider, according to CS-LSA as light sport aircraft and LTF-UL-2019 as ultralight aircraft. The V-24-I is a four-seat, double engine, low plane, composite aircraft. It equipped with Rotax 912 engines with total fuel consumption 40 l/hour (gasoline fuel).

Fig. 4.5 – Softex Aero VP-12

Fig. 4.6 – Softex Aero VP-24-I

In Ukraine based another companies engaged in ultralight aircraft industry, but due to the fact that they are at the stage of first prototypes building or certification, they not included in this list.

5.2 Specifics of ultralight aircraft impact into environment

The most's of ultralight aircraft use piston engine type in a power plant and the most of them is Rotax engines, another part of planes equipped with Lycoming, it even may be some deeply modified motorcycle or car engine.

Currently the most popular is Rotax 912, four-stroke, four-cylinder with carburetor mixture formation engine. Fuel is motor gasoline with an octane rating of at least 95 according to the research method (85 for the motor). Now it has few modification which varies by power, fuel consumption, certification, etc.

In 2012 Rotax Powertrains presented a new modification of engine called 912iS, which is marketing as an eco-engine, it more expensive (about 20 percent premium over the legacy 912 series). But it's more efficient engine providing better takeoff characteristics (high rate of climb and shorter takeoff distance) and increased cruising speed, includes sophisticated self-diagnostics. (Rotax has developed software that will run on PCs to download fault codes and operating data in plain language.) This will be useful during

annular inspections and resource extension. It also can provide useful information to the pilot by showing useful data on compatible avionics. Rotax 912iS can be on 20 percent more efficient than classic 912. That's the difference between 15.9 l/hour and 12.9 l/hour in cruise. A typical 912 spits out 38.6 kg of CO2 per hour compared to 30.8 kg for the 912iS, which is very important parameter in European countries, where the isue of reducing CO2 emissions is a priority.

Last year electric power plant aircraft development trend is gaining popular. Many aircraft manufacturing companies presents a new configurations of their light planes which equipped with electric engines, which makes it zero emission vehicle. Also some enthusiasts install electric power plant on their experimental aircraft's, as example, Yuri Yakovlev a head designer of Aeroprakt company, who installed electric engine on his A-8 aircraft, which was previously designed for piston engine (Fig. 4.7).

Fig. 4.7 – Aeroprakt A-8 with electric power plant

Such aircraft's in most cases has less maximum flight distance and time in comparison to their piston analogs, although electric motors have reached high power with low weight, and their efficiency can be more than 95%, the ratio of energy capacity to

mass of batteries leaves much to be desired, which makes it application difficult and ineffective on big airliners, but their use is justified in light and ultralight aircraft's where flight hour cost can be significantly decreased, and it's a good alternative for flight schools, agriculture industry etc. Electrical power plant is also a good solution for motor gliders or motor hang gliders.

Another direction in development of zero emission aviation, is hydrogen power plant. Brazilian aircraft manufacturer Embraer unveiled Energia, a family of new "green" aircraft that use renewable energy engines. One of the concepts is Energia H2, with capacity 9 people and Range up to 400 km, where hydrogen will be the fuel. Expected to be ready by 2035. In ultralight aviation, the hydrogen fuel plant has not yet become widespread, but it is planned to build serial aircraft in the coming years.

Conclusion to the Part 4

Over the past hundred years, environmental pollution has increased with various emissions. Taking this into account, more and more new technologies appear to reduce the emission of harmful substances into the atmosphere. This trend has also affected ultralight aircraft engines. Such big companies as Rotax Powertrains or Lighcoming created a new series of eco-engines. Rotax 912iS was reviewed in this part as example of new eco-engine, considered its performances, emissions and fuel consumption. Reviewed a new typed of zero-emission engines, whose market may grow significantly in the near future.

GENERAL CONCLUSION

Active flow control systems for lift increasing differ from each other in the features of the physical effect on the flow around the wing, the magnitude of the resulting aerodynamic effect, structural complexity, etc. Therefore, the choice of such system for implementation on an aircraft should be carried out taking into account a number of factors:

- the main purpose of system (improvement of the takeoff and landing, maneuvering or cruising characteristics of the aircraft);
- changes in other aerodynamic characteristics (drag, pitching moment) at given values of the lift coefficient;
- energy consumption required to achieve a given value of lift, or energy efficiency;
- the structural complexity of the system and its mass characteristics;
- the operational characteristics of the system;

There are many limitation should be considered for active flow control system in ultralight aircraft design, which have no enough powerful compressed air source such as in aircraft with gas turbine engines. Also such system should be enough light and cost effective. The comparative analysis of these systems made it possible to draw the main general conclusions about the advantages and disadvantages of each system and give generalized recommendations for selection in which plasma actuator was selected as one of the most promising.

The main task of this work was the development of plasma actuator system for an existing aircraft and to provide recommendations for further designs. To carry out this work, wing geometry of Aeroprakt A20 was analyzed by fulfillment of ANSYS simulations which showed transition points, which can be used to define location of plasma actuators. Considered other airfoils, which can be used in ultralight aircraft design, performed its analysis in XFLR5 software. Davis B24 airfoil was analytically defined as promising airfoil for use in combination with active flow control systems. Based on electrical schemes of existing light aircraft's, proposed solution for plasma actuator system integration, its block diagram and operation principle. Developed plasma generator can be easily installed on aircraft and connected to other avionics units and control panel through CANaerospace bus.

Theoretical calculations of plasma actuators effectiveness and influence on flow are difficult to perform, their results can very significantly from real conditions. For this reason, a number of experimental equipment has been developed and assembled for further investigations. It includes high voltage μs pulse plasma generator, high voltage AC inverter, control module for generators and specialized aerodynamic scales. In accordance with the requirements, basic tests of pulse generator driver board were conducted, which shows excellent results and has only 18ns and 63ns rise and fall time respectively. Aerodynamic scales was tested on static load measurement accuracy and showed that error not exceeds 2g in measurement range 0-2kg force. For further investigations, tests in wind tunnel is required.

Since tests should be performed at the aerodynamic laboratory by engineer, working conditions must comply with established standards. In the part on labor protection, regulatory documents were examined that regulate the parameters for the workplace and the general harmful factors that an engineer may be exposed to in the process of performing work tasks. Also, the required amount of natural light was calculated, which corresponds to the actual working conditions. In terms of environmental protection, Ukrainian ultralight aircraft manufacturers were considered as well as power plants which they use and it’s influence on environment.

REFERENCES

1 Арнольдов В.Н., Серебрийский Я.М., Чутаев А. С. Аэродинамические характеристики самолетов с управлением пограничным слоем на режимах взлета и посадки. Руководство для конструкторов – Москва: БРЭ, ЦАГИ. 1966. – 455 с.

2 Петров А.В. Энергетические системы увеличения подъемной силы. ЦАГИ — основные этапы научной деятельности 1968–1993 – Москва: Наука–Физматлит, 1996. – 404 с.

3 Золотько Е.М., Мартыхина Ю.С. Экспериментальные исследования по при менению управления пограничным слоем (УПС) на закрылках и органах управления самолетов с ТВД с целью улучшения их взлетно-посадочных характеристик – Москва: Труды ЦАГИ. 1965. – 305 с.

4 Арнольдов В.Н., Петров А.В. Управление пограничным слоем на закрылках и зависающих элеронах модели транспортного самолета – Москва: Труды ЦАГИ. 1973. – 45 с.

5 Бюшгенс Г.С. Аэродинамика, устойчивость и управляемость сверхзвуковых самолетов – Москва: Наука–Физматлит. 1998. – 816 с.

6 Петров А.В., Чижов С.И. Продольная балансировка самолета с помощью дополнительных балансировочных крыльев на режимах взлета и посадки – Москва: Труды ЦАГИ, 1978. – 89 с.

7 Ружицкий Е.И. Безаэродромная авиация. – М.: Оборониз. 1959. – 152 с.

8 Korbacher G. K., Sridhar K. A review of the jet flap. UTIA Review No. 14. 1960. – 30 с.

9 Чжен П. Управление отрывом потока – Москва: 1979. – 552 с.

10 R.D. Joslin, G.S. Jones. Applications of circulation control technology. Progress in astronautics and aeronautics. Vol. 214. AIAA, 2006. – 55 с.

11 McCormick B.W. Aerodinamics of V/STOL flight. New York – London, 1967. – 55 с.

12 Sears, W. Magnetohydrodynamic Effects in Aerodynamic Flows. ARS Journal, June 1959. – 397–406 с.

13 Куликовский А.Г., Любимов Г.А. Магнитная гидродинамика – Москва: Физматгиз. 1962. – 246с.

14 Горшков В.А., Климов А.И., Мишин Г.И., и др. Распространение ударных волн в плазме тлеющего разряда при наличии магнитного поля. Письма в ЖТФ. 1984. Т.54. Вып.5. – 995с.

15 Kolesnichenko Yu. F. 2000 2nd Workshop on Magneto-Plasma-Aerodynamics in Aerospace Applications, Moscow, April 2000.

16 Георгиевский П.Ю., Левин В.А. Управление обтеканием различных тел с

помощью локализованного подвода энергии в сверхзвуковой набегающий поток – Москва: РАН. МЖГ. 2003. – 167с.

17 Klimov, V. Bityurin, A. Bocharov, I. Moralev, B. Tolkunov, and P. Kazansky Surface HF Discharge in Airflow 40th AIAA Plasmadynamics and Lasers Conference. 22 - 25 Jun 2009, San Antonio, Texas, AIAA-2009-4073.

18 M. Forte, J. Jolibois, F. Baudoin, E. Moreau, G. Touchard, M. Cazalens, Optimization of a dielectric barrier discharge actuator and nonstationary measurements of the induced flow velocity-application to airflow control, in: 3rd AIAA Flow Control Conference, Paper Number AIAA, 2006, pp. 2006–2863

19 R. Erfani, T. Erfani, S.V. Utyuzhnikov, K. Kontis, Optimisation of multiple encapsulated electrode plasma actuator, Aerosp. Sci. Technol. 26 (1) (2013) 120–127.

20 R. Hippler, H. Kersten, M. Schmidt, K.H. Schoenbach, Low Temperature Plasmas: Fundamentals, Technologies and Techniques, vol. 1, Wiley-VCH, 2008.

21 R. Erfani, H. Zare-Behtash, K. Kontis, Plasma actuator: influence of dielectric surface temperature, Exp. Therm. Fluid Sci. 42 (2012) 258–264.

22 J.R. Roth, X. Dai, Optimization of the aerodynamic plasma actuator as an electrohydrodynamic (EHD) electrical device, in: 44th AIAA Aerospace Sciences Meeting and Exhibit, Reno, Paper Number AIAA-2006-1203, 2006.

23 M. Han, J. Li, Z. Niu, H. Liang, G. Zhao, and W. Hua, “Aerodynamic performance enhancement of a flying wing using nanosecond pulsed DBD plasma actuator,” Chin. J. Aeronaut. 28, 377 (2015).

24 Rasool Erfani, Hossein Zare-Behtash, Craig Hale, Konstantinos Kontis. Development of DBD plasma actuators: The double encapsulated electrode. 2014

25 Karuskevich M.V., Zakiev V.I. Aviation and space rocket technology // Master degree thesis method guide. – K.: NAU, 2021. – 32 p.